Networks and Heterogeneous Media

https://www.aimspress.com/journal/nhm

NHM, 21(2): 669–692.
DOI: 10.3934/nhm.2026029
Received: 03 January 2026
Revised: 01 March 2026
Accepted: 10 March 2026
Published: 24 April 2026

Research article

Three-wave, rogue wave and interaction solutions of the (2+1)-dimensional generalized Hirota-Satsuma-Ito-Shallow-Water-Wave-like equation

Shijie Deng[1], **Bo Tang**[2,1,3,*], **Wenjing Yang**[1], **Kaili Liu**[1] **and Huawei Wu**[2,4]

[1] School of Mathematics and Statistics, Hubei University of Arts and Science, Xiangyang 441053, China

[2] Hubei Key Laboratory of Power System Design and Test for Electrical Vehicle, Hubei University of Arts and Science, Xiangyang 441053, China

[3] School of Mathematics and Computational Science, Xiangtan University, Xiangtan 411105, China

[4] School of Automotive and Traffic Engineering, Hubei University of Arts and Science, Xiangyang 441053, China

* **Correspondence:** Email: tangbo@hbuas.edu.cn.

Abstract: In this article, we focused on the bilinear neural network method to obtain the exact solutions of the (2+1)-dimensional generalized Hirota-Satsuma-Ito-Shallow-Water-Wave-like equation. This method can also be applied to solve other nonlinear partial differential equations (NPDEs). Relying on Hirota bilinear transformation and Bell polynomial theories, we successfully constructed one-hidden-layer and multiple-hidden-layers models with assigned activation functions. Thereby, we derived many exact solutions for this equation including three-wave, rogue wave, and interaction solutions. To intuitively reflect features of these solutions, we depicted their three-dimensional, density, and curve graphs.

Keywords: bilinear neural network method; Hirota bilinear transformation; Bell polynomial; (2+1)-dimensional nonlinear evolution equation; exact solutions

1. Introduction

Nonlinear partial differential equations (NPDEs) are conventionally applied to depict complex phenomena across multiple fields, including mechanics, control systems, ecological systems and economic dynamics. Hirota and Satsuma first proposed the equation named the Hirota-Satsuma equation, which described the propagation of long-wave motions in shallow water [1]. With the in-depth study of nonlinear equations, some scholars have further studied the solutions of this equation. For example, Shang utilized the extended hyperbolic function method to find some exact explicit

solutions to the Hirota-Satsuma equation [2]. Wang et al. employed the Hirota method and Wronskian technique to get the solutions for the Hirota-Satsuma equation [3]. For analyzing the propagation of shallow water waves, Hirota and Satsuma proposed the Hirota-Satsuma-Ito (HSI) equation and Hirota-Satsuma-Shallow-Water-Wave equation [4, 5]. Later, some scholars studied the soliton solutions for the equations [6–8]. Also, Ma et al. researched the lump solutions of the (2+1)-dimensional generalized HSI equation based on Hirota bilinear formulation [9]. Subsequently, Liu et al. successfully obtained the lumps, line solitons, periodic solitons, and interaction solutions for this equation [10]. Then, Khaliq et al. adopted the $\frac{G'}{G'+G+A}$-expansion method to obtain exact solutions to this equation, such as kink and lump solutions [11]. In recent years, many scholars have introduced other methods to derive the exact solutions of NPDEs, such as the Darboux transformation [12–14], Painlevé analysis [15], Hirota bilinear method [16, 17], Lie symmetry analysis [18], generalized $\left(\frac{G'}{G}\right)$-expansion method [19], and unified solver method [20]. Among them, some scholars have investigated the exact solutions and dynamical behaviors of fractional-order evolution equations [21, 22]. More recently, Zhang et al. formulated the bilinear neural network method (BNNM) [23] and bilinear residual network method (BRNM) [24] to get the exact solutions of NPDEs. The methods provide a universal tensor formula that covers almost all post-bilinearization function construction methods for solving NPDEs. By adjusting activation functions, weights, and thresholds, it can derive abundant exact analytical solutions for diverse nonlinear systems without redefining the solution framework. After that, many scholars have employed the methods to obtain solutions to numerous equations [25–27]. Besides, other neural network methods have been proposed to characterize complex nonlinear dynamic phenomena of NPDEs. For example, Wang et al. first embedded the solutions of the fractional Riccati equation into neural networks to establish the fractional sub-equation neural networks (fSENNs) model and successfully obtained the exact solutions for several classes of fractional partial differential equations [28]. Zhang et al. combined neural networks with symbolic computation to obtain the exact solutions without relying on bilinear transformations, which provides a new idea for solving NPDEs [29]. Xie et al. developed a novel neural network–symbolic computation approach and successfully derived multiple groups of solutions for NPDEs [30].

In addition, many scholars have extended neural network methods to fields like finance and transportation. For instance, Yin et al. incorporated a multi-head attention mechanism into the spatiotemporal convolutional network as an effective extension module [31] and designed the car-following-informed neural network (CFINN), which can not only reduce prediction errors but also realize the calibration of model parameters through continuous research [32]. In recent years, the physics-informed neural network (PINN) has been extensively adopted in diverse fields. Chen et al. constructed the PINN to solve the coupled pricing system for the up-and-out call option and analyzed the corresponding volatility surface [33]. The results demonstrate that the PINN exhibits high efficiency in financial derivative pricing. Subsequently, Chen et al. improved the framework and developed the extended physics-informed neural network (ePINN) framework with higher accuracy and better robustness than the traditional PINN [34]. Guo et al. incorporated single-layer Kolmogorov-Arnold networks (KANs) into the downstream framework of PINNs and adopted an alternating training scheme with sparse regression algorithms [35]. Different from the BNNM, this method does not require excessive constraints, thus greatly simplifying the computational process. Based on the PINN, Han et al. proposed a novel variable coefficient-informed neural network (VCINN), which combines the PINN with the constraint of coefficients to address the inverse problem of variable-coefficient partial

differential equations in fluid dynamics [36]. In the field of intelligent transportation, Su et al. embedded an adaptive macro model for mixed traffic flow into the structure of the PINN, which can characterize physical features and laws with only a small amount of data [37].

In this article, we mainly concentrate on the following (2+1)-dimensional generalized Hirota-Satsuma-Ito-Shallow-Water-Wave (gHSISWW) equation:

$$w_{xxxt} + 3(w_x w_t)_x + \delta_1 w_{yt} + \delta_2 w_{xx} + \delta_3 w_{xy} + \delta_4 w_{xt} + \delta_5 w_{yy} = 0. \tag{1.1}$$

The generalized bilinear form is defined as listed below:

$$\begin{aligned} &D^w_{p,x} D^s_{p,y} D^h_{p,t} f(x,y,t) g(x',y',t') = \\ &(\frac{\partial}{\partial x} + \beta \frac{\partial}{\partial x'})^w (\frac{\partial}{\partial y} + \beta \frac{\partial}{\partial y'})^s (\frac{\partial}{\partial t} + \beta \frac{\partial}{\partial t'})^h f(x,y,t) g(x',y',t')|_{x'=x,y'=y,t'=t}, \end{aligned} \tag{1.2}$$

where w, s, h are the integers with values that are not less than zero. For an integer q, the qth power of β is defined by $\beta^q = (-1)^{r(q)}$, if $q \equiv r(q) \bmod p$ with $0 \le r(q) < p$ [38, 39].

Utilizing the transformation [40]:

$$w(x,y,t) = 2(\ln f(x,y,t))_x, \tag{1.3}$$

when p is set to 3, the generalized bilinear form corresponding to Eq (1.1) is able to be expressed as follows:

$$\begin{aligned} T &= (D_{3,t} D^3_{3,x} + \delta_1 D_{3,t} D_{3,y} + \delta_2 D^2_x + \delta_3 D_{3,x} D_{3,y} + \delta_4 D_{3,t} D_{3,x} + \delta_5 D^2_y) f \cdot f \\ &= 3 f_{xt} f_{xx} + \delta_1 f f_{yt} - \delta_1 f_t f_y + \delta_2 f f_{xx} - \delta_2 f_x^2 + \delta_3 f f_{xy} - \delta_3 f_x f_y + \delta_4 f f_{xt} \\ &\quad - \delta_4 f_t f_x + \delta_5 f f_{yy} - \delta_5 f_y^2 \\ &= 0. \end{aligned} \tag{1.4}$$

Based on the HSI equation and the shallow water wave equation, the generalized bilinear equation (1.4) is transformed into the (2+1)-dimensional gHSISWW-like equation via the Bell polynomials [39, 41] and transformation (1.3) by computing $\left[\frac{T}{f^2}\right]_x$ with $f = \mathrm{e}^{\frac{\int w\,dx}{2}}$. Its detailed derivation is presented in Appendix A.

$$\begin{aligned} &3w^3 w_t + 9w^2 w_x \int w_t\,dx + 6w w_{xx} \int w_t\,dx + 18 w w_t w_x + \\ &6w_x^2 \int w_t\,dx + 12 w_t w_{xx} + 6w^2 w_{xt} + 12 w_x w_{xt} + 8\delta_1 w_{yt} + \\ &8\delta_2 w_{xx} + 8\delta_3 w_{xy} + 8\delta_4 w_{xt} + 8\delta_5 w_{yy} = 0. \end{aligned} \tag{1.5}$$

Due to the increased number of nonlinear terms, Eq (1.5) can exhibit richer dynamics and more interesting physical phenomena. In contrast to the classical HSI equation and its generalized form [9–11], which are dominated by quadratic and cubic nonlinear terms with relatively simple coupling structures, Eq (1.5) incorporates additional high-order nonlinear interaction terms and mixed polynomial-exponential nonlinear couplings. This structural refinement fundamentally modifies the balance between nonlinearity and dispersion in the system, leading to differences in both solution types and their dynamic behaviors.

To attain improved insight into the physical mechanisms, it will be necessary to investigate the solutions of this equation. It is precisely for this purpose that we made use of this method to find some exact solutions to Eq (1.5).

Below is outlined the structure of this article. In Section 2, a brief introduction to the BNNM is presented. In Section 3, we build a model with two hidden layers to derive the three wave solutions of Eq (1.5) based on this method. In Sections 4 and 5, we construct a two-hidden-layer model and a one-hidden-layer model, respectively, to derive the rogue wave solutions and the interaction solutions of this equation. Thereafter, we plot three-dimensional, density, and curve diagrams, which illustrate the properties of these solutions. In Section 6, we summarize the outcomes of the study.

2. Bilinear neural network method

The BNNM can adapt to nonlinearity and high dimensionality, and also possesses high computational efficiency and wide application, remedying the limitations of traditional methods in dealing with complex nonlinear systems. The characteristics will be presented in the subsequent analysis of three types of models. Next, aiming to get the exact solutions for Eq (1.5), in the framework as shown in Figure 1 of nonlinear neural networks, we will establish the tensor formula as follows:

$$f = \rho_{l_n,r}\phi_{l_n}(\xi_{l_n}) + a_{l_n}, \tag{2.1}$$

where $\rho_{l_n,f}$ is the coefficient which measures the weight between neuron l_n and function f, ϕ refers to the generalized activation function, and $a_{l_i}(i = 1, 2, ..., n)$ are constants. It is noticed that $\phi_{l_n}(\xi) \geq 0$. For $l_n = \{k_{n-1} + 1, k_{n-1} + 2, ..., n\}$, it denotes the region of the nth layer in the neural network model. Also, the definition of parameter ξ_{l_n} is as follows:

$$\xi_{l_i} = \rho_{l_i,l_{i-1}}\phi_{l_{i-1}}(\xi_{l_{i-1}}) + b_{l_i}, i = 1, 2, ..., n, \tag{2.2}$$

where $l_0 = \{x, y, \ldots, t\}, l_1 = \{1, 2, \ldots, k_1\}, l_i = \{k_{i-1} + 1, k_{i-1} + 2, ..., k_i\}(i = 2, ..., n - 1)$, and b_{l_i} are constants. The specific operational procedure of this method can be referred to in [23, 27, 41].

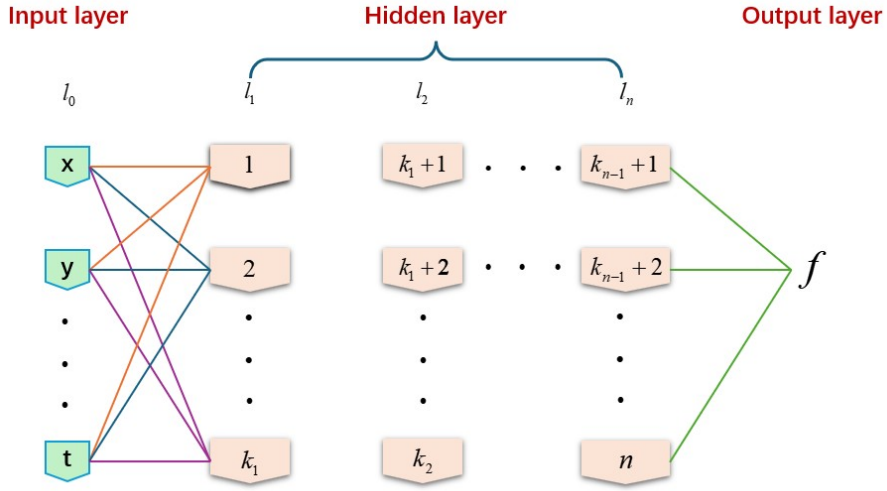

Figure 1. Neural network tensor model for Eq (2.1).

3. Three-wave solutions

For this section, we will investigate the three-wave solutions of Eq (1.5). We established a "3-2-3-1" model by setting the hidden layers $l_1 = \{1, 2\}$ and $l_2 = \{3, 4, 5\}$ as presented in Figure 2. When selecting the appropriate activation functions as $\phi_1(\xi_1) = \xi_1, \phi_2(\xi_2) = \xi_2, \phi_3(\xi_3) = e^{\xi_3}, \phi_4(\xi_4) = \sin(\xi_4), \phi_5(\xi_5) = \cos(\xi_5)$ [42], we obtain the function as follows:

$$\begin{cases} f = \rho_{3,r}\phi_3(\xi_3) + \rho_{4,r}\phi_3(-\xi_3) + \rho_{5,r}\phi_4(\xi_4) + \rho_{6,r}\phi_5(\xi_5) + a, \\ \xi_3 = \rho_{3,1}\phi_1(\xi_1) + \rho_{3,2}\phi_2(\xi_2) + b_3, \\ \xi_4 = \rho_{4,1}\phi_1(\xi_1) + \rho_{4,2}\phi_2(\xi_2) + b_4, \\ \xi_5 = \rho_{5,1}\phi_1(\xi_1) + \rho_{5,2}\phi_2(\xi_2) + b_5, \\ \xi_1 = \varepsilon_1 x + \varepsilon_2 y + \varepsilon_3 t + b_1, \\ \xi_2 = \varepsilon_4 x + \varepsilon_5 y + \varepsilon_6 t + b_2, \end{cases} \tag{3.1}$$

where a and $b_k (k = 1, 2, 3, 4, 5)$ are constants.

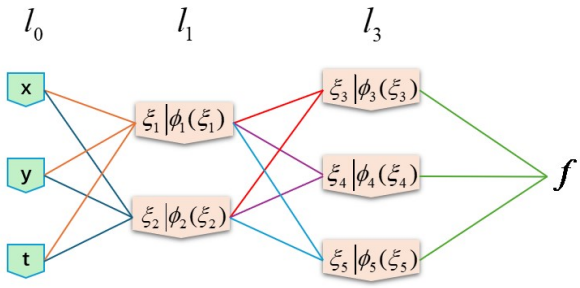

Figure 2. "3-2-3-1" model for Eq (2.1).

Remark 1: Based on an analysis of the construction methods of classical neural network models, the "3-2-3-1" model adopted in this equation actually represents the hidden layers in the form of composite functions. Through analysis, we find that this model is equivalent to the classical "3-3-1" model when $\phi_1(\xi_1) = \xi_1, \phi_2(\xi_2) = \xi_2$. Upon setting $\phi_1(\xi_1) \neq \xi_1, \phi_2(\xi_2) \neq \xi_2$, a "3-2-3-1" model can be constructed to derive many new three-wave solutions.

Putting Eq (3.1) into Eq (1.4) and setting the coefficients of each term to zero, we derive a system of equations via Mathematica and obtain the following two types of solutions:

Case 3.1:

$$\begin{aligned} &\varepsilon_1 = -\frac{\varepsilon_4\rho_{3,2}}{\rho_{3,1}}, \varepsilon_2 = -\frac{\varepsilon_5\rho_{3,2}}{\rho_{3,1}}, \varepsilon_6 = -\frac{\varepsilon_3\rho_{4,1}}{\rho_{4,2}}, \delta_3 = \frac{-\delta_2\varepsilon_4^2 - \delta_5\varepsilon_5^2}{\varepsilon_4\varepsilon_5}, \\ &\delta_4 = -\frac{\delta_1\varepsilon_5}{\varepsilon_4}, \rho_{5,2} = \frac{\rho_{3,2}\rho_{5,1}}{\rho_{3,1}}. \end{aligned} \tag{3.2}$$

Case 3.2:

$$\begin{aligned}
&\varepsilon_3 = -\frac{\varepsilon_6\rho_{5,2}}{\rho_{5,1}}, \varepsilon_4 = -\frac{\varepsilon_1\rho_{3,1}}{\rho_{3,2}},\\
&\varepsilon_5 = \frac{-\delta_5\varepsilon_2\rho_{3,1}\rho_{5,1} - \delta_1\varepsilon_6\rho_{3,2}\rho_{5,1} + \delta_1\varepsilon_6\rho_{3,1}\rho_{5,2}}{\delta_5\rho_{3,2}\rho_{5,1}},\\
&\delta_2 = -\frac{\left(\delta_5\varepsilon_2\rho_{5,1} - \delta_1\varepsilon_6\rho_{5,2}\right)\left(\delta_3\varepsilon_1\rho_{5,1} + \delta_5\varepsilon_2\rho_{5,1} - \delta_1\varepsilon_6\rho_{5,2}\right)}{\delta_5\varepsilon_1^2\rho_{5,1}^2},\\
&\delta_4 = -\frac{\delta_1\left(-\delta_3\varepsilon_1\rho_{5,1} - \delta_5\varepsilon_2\rho_{5,1} + \delta_1\varepsilon_6\rho_{5,2}\right)}{\delta_5\varepsilon_1\rho_{5,1}},\\
&\rho_{4,1} = \frac{\rho_{4,2}\rho_{5,1}}{\rho_{5,2}}.
\end{aligned} \tag{3.3}$$

By plugging Eqs (3.2) and (3.3) into Eq (3.1) and using transformation Eq (1.3), we can acquire the following three-wave solutions:

$$w_1 = \frac{2\varepsilon_4\Omega_3\left(\rho_{3,1}\rho_{4,2} - \rho_{3,2}\rho_{4,1}\right)\cos\left(\Omega_1\right)\rho_{5,r}}{\rho_{3,1}\left(\Omega_3\left(\sin\left(\Omega_1\right)\rho_{5,r} + \cos\left(\Omega_2\right)\rho_{6,r} + a\right) + \rho_{3,r}\Omega_3^2\mathrm{e}^{-2\Omega_4} + \rho_{4,r}\mathrm{e}^{2\Omega_4}\right)}, \tag{3.4}$$

where

$$\begin{cases}
\Omega_1 = b_1\rho_{4,1} + b_2\rho_{4,2} + \varepsilon_4\rho_{4,2}x - \frac{\varepsilon_4\rho_{3,2}\rho_{4,1}}{\rho_{3,1}}x + \varepsilon_5\rho_{4,2}y - \frac{\varepsilon_5\rho_{3,2}\rho_{4,1}}{\rho_{3,1}}y + b_4,\\
\Omega_2 = b_1\rho_{5,1} + \frac{b_2\rho_{3,2}\rho_{5,1}}{\rho_{3,1}} + \varepsilon_3\rho_{5,1}t - \frac{\rho_{5,1}}{\rho_{3,1}}\Omega_4 + b_5,\\
\Omega_3 = \mathrm{e}^{b_1\rho_{3,1}+b_2\rho_{3,2}+\varepsilon_3\rho_{3,1}t+\Omega_4+b_3},\\
\Omega_4 = \frac{\varepsilon_3\rho_{3,2}\rho_{4,1}}{\rho_{4,2}}t.
\end{cases} \tag{3.5}$$

In addition,

$$w_2 = \frac{2\varepsilon_1\Omega_1\left(\rho_{3,1}\rho_{5,2} - \rho_{3,2}\rho_{5,1}\right)\left(\rho_{5,2}\sin\left(\Omega_3\right)\rho_{6,r} - \rho_{4,2}\cos\left(\Omega_2\right)\rho_{5,r}\right)}{\rho_{3,2}\rho_{5,2}\left(\Omega_1\left(\sin\left(\Omega_2\right)\rho_{5,r} + \cos\left(\Omega_3\right)\rho_{6,r} + a\right) + \Omega_1^2\rho_{3,r} + \rho_{4,r}\right)}, \tag{3.6}$$

where

$$\begin{cases}
\Omega_1 = \mathrm{e}^{b_1\rho_{3,1}+b_2\rho_{3,2}+\varepsilon_6\rho_{3,2}t-\Omega_6+b_3},\\
\Omega_2 = -\rho_{4,2}\left(\Omega_4 + \Omega_5\right) + b_2\rho_{4,2} + b_4,\\
\Omega_3 = b_1\rho_{5,1} + b_2\rho_{5,2} + \varepsilon_1\rho_{5,1}x + \varepsilon_2\rho_{5,1}y - \Omega_5\rho_{5,2} + b_5,\\
\Omega_4 = -\frac{b_1\rho_{5,1}}{\rho_{5,2}} - \frac{\varepsilon_1\rho_{5,1}}{\rho_{5,2}}x - \frac{\varepsilon_2\rho_{5,1}}{\rho_{5,2}}y,\\
\Omega_5 = \frac{\varepsilon_1\rho_{3,1}}{\rho_{3,2}}x - \frac{\delta_1\varepsilon_6\rho_{3,1}\rho_{5,2}}{\delta_5\rho_{3,2}\rho_{5,1}}y + \frac{\varepsilon_2\rho_{3,1}}{\rho_{3,2}}y + \frac{\delta_1\varepsilon_6}{\delta_5}y,\\
\Omega_6 = \frac{\varepsilon_6\rho_{3,1}\rho_{5,2}}{\rho_{5,1}}t - \frac{\delta_1\varepsilon_6\rho_{3,1}\rho_{5,2}}{\delta_5\rho_{5,1}}y + \frac{\delta_1\varepsilon_6\rho_{3,2}}{\delta_5}y.
\end{cases} \tag{3.7}$$

The graphs in Figures 3 and 4 are generated to illustrate characteristics of the three-wave solutions. By observing three-dimensional and density plots, we learn that the wave crests and troughs present a distinct sawtooth profile. Figure 3(c) shows that the wave field evolves periodically along the positive y-axis with the increase of the time variable. In Figure 4(c), we can also clearly see that the wave shows a horizontal tendency of the waveform as time decreases. Such dynamic behaviors are the direct physical manifestation of the balance between nonlinearity and dispersion in the equation, which is consistent with the intrinsic propagation characteristics of three-wave solutions in nonlinear shallow water wave systems, reflecting the mutual modulation and energy exchange among the three interacting waves [43].

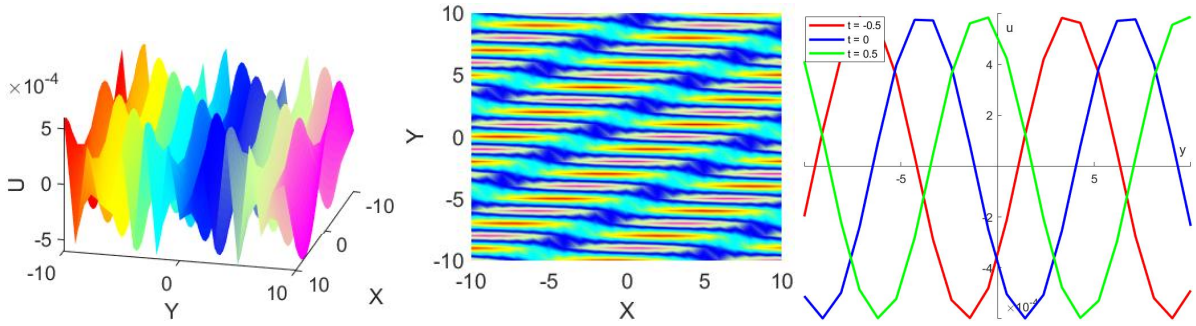

(a) (b) (c)

Figure 3. Three-wave solution w_1 with: $\varepsilon_3 = -1, \varepsilon_4 = 2, \varepsilon_5 = -3, \rho_{3,1} = \frac{1}{2}, \rho_{3,2} = 3, \rho_{4,1} = 1, \rho_{4,2} = 3, \rho_{5,1} = 2, \rho_{3,r} = 4, \rho_{4,r} = 3, \rho_{5,r} = 2, \rho_{6,r} = 5, a = 2, b_1 = 2, b_2 = -3, b_3 = -\frac{1}{2}, b_4 = 3, b_5 = \frac{3}{2}, t = -2$. (a): Three-dimensional plot; (b): density plot; (c): curve plots.

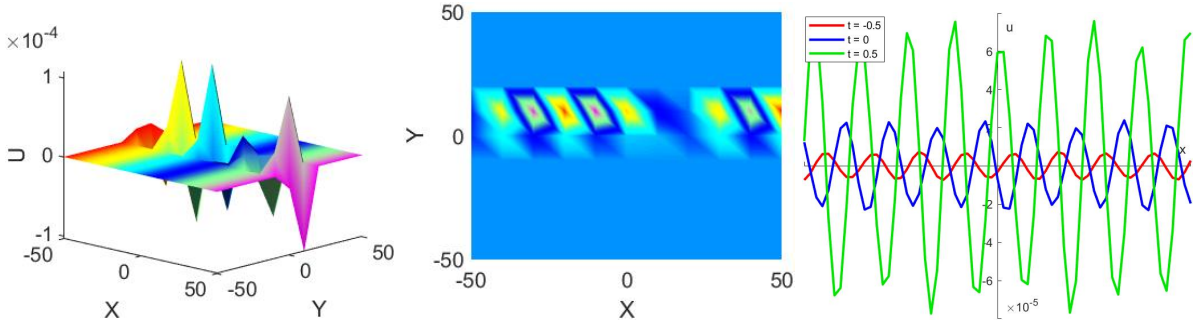

(a) (b) (c)

Figure 4. Three-wave solution w_2 with: $\varepsilon_1 = 2, \varepsilon_2 = 1, \varepsilon_6 = 2, \delta_1 = 2, \delta_5 = 4, \rho_{3,1} = 1, \rho_{3,2} = -4, \rho_{4,2} = 1, \rho_{5,1} = -3, \rho_{5,2} = 5, \rho_{3,r} = -3, \rho_{4,r} = 2, \rho_{5,r} = -1, \rho_{6,r} = 2, a = 3, b_1 = -1, b_2 = 3, b_3 = 5, b_4 = 1, b_5 = -2, t = 1$. (a): Three-dimensional plot; (b): density plot; (c): curve plots.

Remark 2: By setting $\phi_1(\xi_1) = {\xi_1}^2, \phi_2(\xi_2) = \mathrm{e}^{\xi_2}$, a new three-wave solution can be derived from the "3-2-3-1" model and the detailed procedure is presented as follows:

After substituting Eq (3.1) with new activation functions into Eq (1.4), we can obtain the solution as follows:

Case 3.3:

$$\begin{aligned} &\varepsilon_1 = 0, \varepsilon_2 = 0, \varepsilon_4 = \frac{\sqrt{\delta_3^2\varepsilon_5^2 - 4\delta_2\delta_5\varepsilon_5^2} - \delta_3\varepsilon_5}{2\delta_2}, \varepsilon_6 = 0, \\ &\delta_4 = \frac{\delta_1\sqrt{\left(\delta_3^2 - 4\delta_2\delta_5\right)\varepsilon_5^2} + \delta_3\delta_1\varepsilon_5}{2\delta_5\varepsilon_5}, \rho_{3,2} = 0, \rho_{4,1} = 0, \rho_{5,1} = 0. \end{aligned} \tag{3.8}$$

Based on transformation Eq (1.3), we can derive following solution by plugging Eq (3.8) into Eq (3.1):

$$w_3 = \frac{e^{\Omega_1+\Omega_5}\Omega_2\Omega_4}{\delta_2\left(e^{2\Omega_5}\rho_{3,r} + \rho_{4,r} + e^{\Omega_5}\left(a+\Omega_3\right)\right)}, \tag{3.9}$$

where

$$\begin{cases} \Omega_1 = b_2 + \frac{x\Omega_4}{2\delta_2} + \varepsilon_5 y, \\ \Omega_2 = \rho_{4,2}\rho_{5,r}\cos\left(e^{\Omega_1}\rho_{4,2} + b_4\right) - \rho_{5,2}\rho_{6,r}\sin\left(e^{\Omega_1}\rho_{5,2} + b_5\right), \\ \Omega_3 = \rho_{5,r}\sin\left(e^{\Omega_1}\rho_{4,2} + b_4\right) + \rho_{6,r}\cos\left(e^{\Omega_1}\rho_{5,2} + b_5\right), \\ \Omega_4 = \sqrt{\left(\delta_3^2 - 4\delta_2\delta_5\right)\varepsilon_5^2} - \delta_3\varepsilon_5, \\ \Omega_5 = \rho_{3,1}\left(b_1 + \varepsilon_3 t\right)^2 + b_3. \end{cases} \tag{3.10}$$

Figure 5 is plotted to reflect the dynamic behavior of solution (3.9). Figure 5(a) shows that the amplitude of the solution exhibits an obvious multi-peak and multi-valley structure. From Figure 5(b), we can observe clear wavy interference fringes. The curve in Figure 5(c) reflects that the profile and amplitude of the solution vary significantly with time. Therefore, this solution exhibits the fundamental physical properties of a three-wave solution.

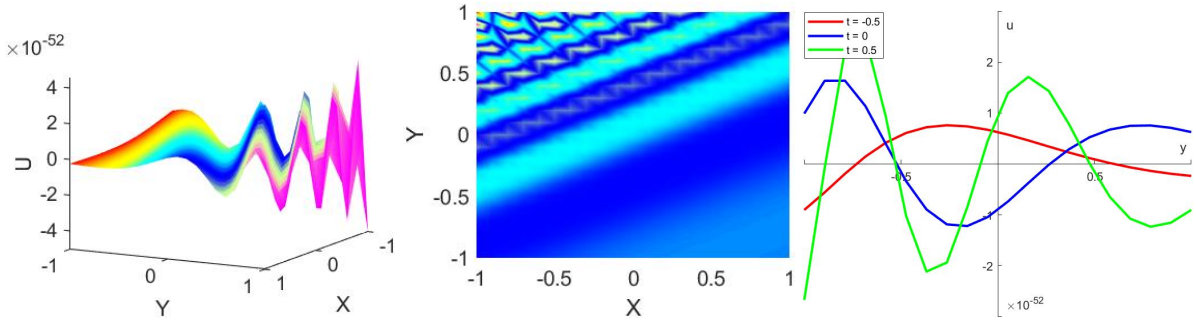

(a) (b) (c)

Figure 5. Three-wave solution w_3 with: $\varepsilon_1 = 1, \varepsilon_5 = 1, \delta_2 = 2, \delta_3 = 3, \delta_5 = 1, \rho_{3,1} = 1, \rho_{4,2} = -1, \rho_{5,2} = 1, \rho_{3,r} = 1, \rho_{4,r} = 3, \rho_{5,r} = 1, \rho_{6,r} = 3, a = -2, b_1 = -1, b_2 = 2, b_3 = 2, b_4 = 5, b_5 = 3, t = -10$. (a): Three-dimensional plot; (b): density plot; (c): curve plots.

4. Rogue wave solutions

Based on reference [42], rogue waves exhibit multiple uniformly distributed crests and troughs, maintaining spatial localization while showing stable temporal periodic evolution, which is a direct result of the balance between nonlinear coupling and dispersive effects in the system. To secure the rogue wave solutions associated with Eq (1.5), this section will add another hidden layer to build a "3-2-2-1" model as shown in Figure 6. Based on Section 3 of reference [24], we can assign the activation functions as $\phi_1(\xi_1) = \xi_1, \phi_2(\xi_2) = e^{\xi_2}, \phi_3(\xi_3) = {\xi_3}^2, \phi_4(\xi_4) = {\xi_4}^2$, and the derived function is shown

as follows:

$$\begin{cases} f = \rho_{3,r}\phi_3(\xi_3) + \rho_{4,r}\phi_4(\xi_4) + a, \\ \xi_3 = \rho_{3,1}\phi_1(\xi_1) + \rho_{3,2}\phi_2(\xi_2) + b_3, \\ \xi_4 = \rho_{4,1}\phi_1(\xi_1) + \rho_{4,2}\phi_2(\xi_2) + b_4, \\ \xi_1 = \varepsilon_1 x + \varepsilon_2 y + \varepsilon_3 t + b_1, \\ \xi_2 = \varepsilon_4 x + \varepsilon_5 y + \varepsilon_6 t + b_2, \end{cases} \tag{4.1}$$

where a and $b_k (k = 1, 2, 3, 4)$ are constants. Following the approach taken in Section 3, putting Eq (4.1) into Eq (1.4), we get the solutions:

Case 4.1:

$$\begin{aligned} &\varepsilon_1 = 0, \varepsilon_2 = -\frac{\varepsilon_3\delta_1}{\delta_5}, \varepsilon_4 = -\frac{\varepsilon_5\delta_4\delta_5}{\delta_1\delta_2}, \varepsilon_6 = 0, \\ &\delta_3 = \frac{\delta_1^2\delta_2 + \delta_4^2\delta_5}{\delta_1\delta_4}, \rho_{3,1} = -\frac{\rho_{4,1}\rho_{4,2}\rho_{4,r}}{\rho_{3,2}\rho_{3,r}}. \end{aligned} \tag{4.2}$$

Case 4.2:

$$\begin{aligned} &\varepsilon_2 = \frac{\varepsilon_1\sqrt{\delta_3^2 - 4\delta_2\delta_5} - \varepsilon_1\delta_3}{2\delta_5}, \varepsilon_3 = 0, \varepsilon_4 = 0, \\ &\varepsilon_5 = \frac{\varepsilon_6\delta_4\sqrt{\delta_3^2 - 4\delta_2\delta_5} - \varepsilon_6\delta_3\delta_4}{2\delta_2\delta_5}, \delta_1 = \frac{\delta_3\delta_4 - \delta_4\sqrt{\delta_3^2 - 4\delta_2\delta_5}}{2\delta_2}, \\ &\rho_{3,2} = -\frac{\rho_{4,1}\rho_{4,2}\rho_{4,r}}{\rho_{3,1}\rho_{3,r}}. \end{aligned} \tag{4.3}$$

In a similar way, under transformation Eq (1.3), we acquire the corresponding rogue wave solutions by substituting Eqs (4.2) and (4.3) into Eq (4.1):

$$w_4 = -\frac{4\delta_4\delta_5\varepsilon_5\left(\rho_{4,2}\rho_{4,r}\Phi_2 + \Phi_1\right)\mathrm{e}^{b_2 - 2\Phi_5 + \varepsilon_5 y}}{\delta_1\delta_2\left(\rho_{3,r}\left(b_3 + \Phi_4\right)^2 + \rho_{4,r}\Phi_3^2 + a\right)}, \tag{4.4}$$

where

$$\begin{cases} \Phi_1 = b_3\rho_{3,2}\rho_{3,r}\mathrm{e}^{\Phi_5} + \rho_{3,2}^2\rho_{3,r}\mathrm{e}^{b_2 + \varepsilon_5 y}, \\ \Phi_2 = \rho_{4,2}\mathrm{e}^{b_2 + \varepsilon_5 y} + b_4\mathrm{e}^{\Phi_5}, \\ \Phi_3 = \rho_{4,2}\mathrm{e}^{b_2 - \Phi_5 + \varepsilon_5 y} + \rho_{4,1}\Phi_6 + b_4, \\ \Phi_4 = \rho_{3,2}\mathrm{e}^{b_2 - \Phi_5 + \varepsilon_5 y} - \frac{\rho_{4,1}\rho_{4,2}\rho_{4,r}}{\rho_{3,2}\rho_{3,r}}\Phi_6, \\ \Phi_5 = \frac{\delta_4\delta_5\varepsilon_5}{\delta_1\delta_2}x, \\ \Phi_6 = b_1 + \varepsilon_3 t - \frac{\delta_1\varepsilon_3}{\delta_5}y. \end{cases} \tag{4.5}$$

In addition,

$$w_5 = \frac{2\varepsilon_1\left(\rho_{3,1}^2\rho_{3,r}\left(2\delta_5\Phi_5 + \delta_3\varepsilon_1 y\right) + \rho_{4,1}^2\rho_{4,r}\left(2\delta_5\Phi_5 + \delta_3\varepsilon_1 y\right) + \Phi_1 + \Phi_2 + \Phi_7\right)}{\delta_5\left(\Phi_3^2\rho_{4,r} + \Phi_4^2\rho_{3,r} + a\right)}, \tag{4.6}$$

where

$$\begin{cases} \Phi_1 = 2b_3\delta_5\rho_{3,1}\rho_{3,r} + 2\varepsilon_1\delta_5\rho_{3,1}^2\rho_{3,r}x - \varepsilon_1\delta_3\rho_{3,1}^2\rho_{3,r}y, \\ \Phi_2 = 2b_4\delta_5\rho_{4,1}\rho_{4,r} + 2\varepsilon_1\delta_5\rho_{4,1}^2\rho_{4,r}x - \varepsilon_1\delta_3\rho_{4,1}^2\rho_{4,r}y, \\ \Phi_3 = \rho_{4,1}\left(b_1 + \Phi_5 + \varepsilon_1 x\right) + \rho_{4,2}\Phi_6 + b_4, \\ \Phi_4 = \rho_{3,1}\left(b_1 + \Phi_5 + \varepsilon_1 x\right) - \frac{\rho_{4,1}\rho_{4,2}\rho_{4,r}}{\rho_{3,1}\rho_{3,r}}\Phi_6 + b_3, \\ \Phi_5 = \frac{\varepsilon_1\left(-\delta_3 + \sqrt{\delta_3^2 - 4\delta_2\delta_5}\right)}{2\delta_5}y, \\ \Phi_6 = \mathrm{e}^{b_2 + \frac{\varepsilon_6\delta_4}{\delta_2}\Phi_5 + \varepsilon_6 t}, \\ \Phi_7 = 2b_1\delta_5\left(\rho_{3,1}^2\rho_{3,r} + \rho_{4,1}^2\rho_{4,r}\right). \end{cases} \tag{4.7}$$

To exhibit characteristics of the rogue wave solutions of Eq (1.5), we designate parameters and generate the following plots as shown in Figures 7 and 8. Through analysis, we can find that the rogue wave solutions exhibit multiple well-distributed wave crests and troughs with significant amplitude fluctuations, manifesting the typical localized oscillation behavior of rogue waves induced by the balance between nonlinearity and dispersion in the system. Figures 7(c) and 8(c) show that the amplitudes and positions of the wave crests and troughs undergo regular adjustments, and obvious oscillations are observed in specific spatial regions with the variation of the time variable.

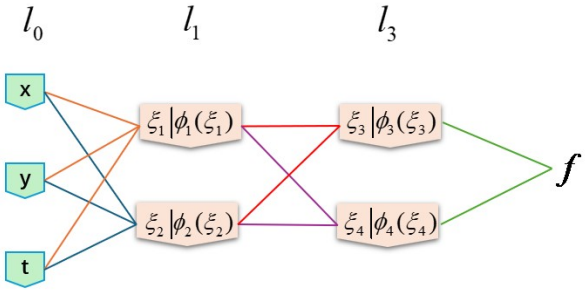

Figure 6. "3-2-2-1" model for Eq (2.1).

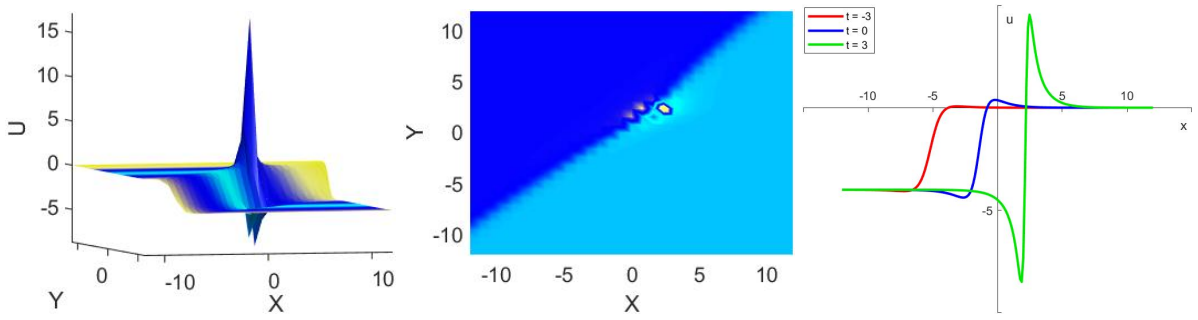

(a) (b) (c)

Figure 7. Rogue wave solution w_4 with: $\varepsilon_3 = -1, \varepsilon_5 = 1, \delta_1 = 1, \delta_2 = -2, \delta_4 = 2, \delta_5 = -1, \rho_{3,2} = -2, \rho_{4,1} = 1, \rho_{4,2} = -1, \rho_{3,r} = 2, \rho_{4,r} = 3, a = -2, b_1 = 2, b_2 = -1, b_3 = 0, b_4 = 3, t = 2$. (a): Three-dimensional plot; (b): density plot; (c): curve plots.

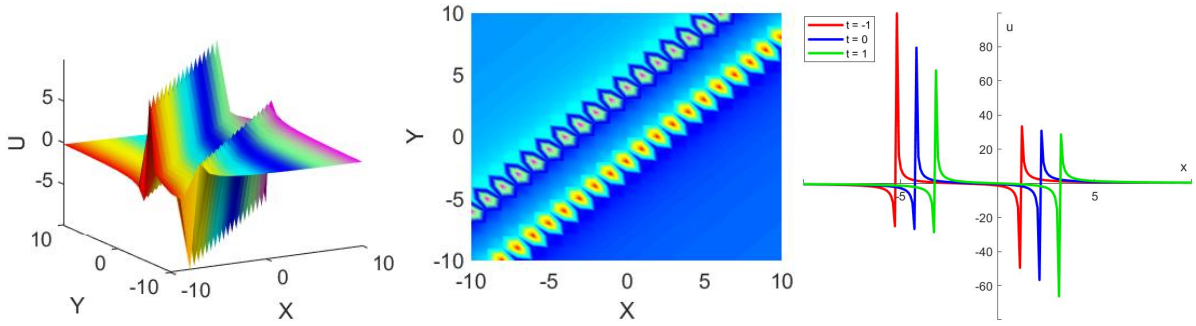

(a) (b) (c)

Figure 8. Rogue wave solution w_5 with: $\varepsilon_1 = 1, \varepsilon_6 = 0, \delta_2 = 2, \delta_3 = 3, \delta_4 = 1, \delta_5 = 1, \rho_{3,1} = 1, \rho_{4,1} = 1, \rho_{4,2} = 2, \rho_{3,r} = -2, \rho_{4,r} = 1, a = -1, b_1 = 1, b_2 = -1, b_3 = 2, b_4 = 4, t = 1$. (a): Three-dimensional plot; (b): density plot; (c): curve plots.

5. Interaction solutions

Turning to this section, we establish the "3-3-1" model, whose input layer is $l_0 = \{x, y, t\}$ and hidden layer is $l_1 = \{1, 2, 3\}$ as shown in Figure 9, to acquire the interaction solutions between the lump and exponential function for Eq (1.5). The specific form of the test function is as follows:

$$\begin{cases} f = \rho_{1,r}\phi_1(\xi_1) + \rho_{2,r}\phi_2(\xi_2) + \rho_{3,r}\phi_3(\xi_3) + a, \\ \xi_1 = \varepsilon_1 x + \varepsilon_2 y + \varepsilon_3 t + b_1, \\ \xi_2 = \varepsilon_4 x + \varepsilon_5 y + \varepsilon_6 t + b_2, \\ \xi_3 = \varepsilon_7 x + \varepsilon_8 y + \varepsilon_9 t + b_3, \end{cases} \tag{5.1}$$

where a and $b_k (k = 1, 2, 3)$ are constants. Also, we select activation functions as $\phi_1(\xi_1) = \xi_1^2$, $\phi_2(\xi_2) = \xi_2^2$, $\phi_3(\xi_3) = e^{\xi_3}$. After inserting Eq (5.1) into Eq (1.4), we acquire the two solutions by solving the obtained coefficient equation system:

Case 5.1:

$$\begin{aligned} &\varepsilon_1 = -\frac{\varepsilon_4\varepsilon_6\rho_{2,r}}{\varepsilon_3\rho_{1,r}}, \varepsilon_5 = \frac{\varepsilon_4\varepsilon_8\varepsilon_3^2\rho_{1,r} + \varepsilon_2\varepsilon_6\varepsilon_7\varepsilon_3\rho_{1,r} + \varepsilon_4\varepsilon_6^2\varepsilon_8\rho_{2,r}}{\varepsilon_3^2\varepsilon_7\rho_{1,r}}, \varepsilon_9 = 0, \\ &\delta_1 = \frac{(\delta_2\varepsilon_7 + \delta_3\varepsilon_8)(\varepsilon_2\varepsilon_3\varepsilon_7\rho_{1,r} + \varepsilon_4\varepsilon_6\varepsilon_8\rho_{2,r})}{\varepsilon_3^2\varepsilon_8^2\rho_{1,r}}, \delta_4 = \frac{\delta_2(\varepsilon_2\varepsilon_3\varepsilon_7\rho_{1,r} + \varepsilon_4\varepsilon_6\varepsilon_8\rho_{2,r})}{\varepsilon_3^2\varepsilon_8\rho_{1,r}}, \\ &\delta_5 = \frac{-\delta_2\varepsilon_7^2 - \delta_3\varepsilon_8\varepsilon_7}{\varepsilon_8^2}. \end{aligned} \tag{5.2}$$

Case 5.2:

$$\begin{aligned} &\varepsilon_1 = -\frac{\delta_4(\varepsilon_3\varepsilon_8 - \varepsilon_2\varepsilon_9)}{\delta_2\varepsilon_8}, \varepsilon_4 = \frac{\delta_4\varepsilon_3(\varepsilon_3\varepsilon_8 - \varepsilon_2\varepsilon_9)\rho_{1,r}}{\delta_2\varepsilon_6\varepsilon_8\rho_{2,r}}, \\ &\varepsilon_5 = \frac{\varepsilon_8\varepsilon_3^2\rho_{1,r} - \varepsilon_2\varepsilon_9\varepsilon_3\rho_{1,r} + \varepsilon_6^2\varepsilon_8\rho_{2,r}}{\varepsilon_6\varepsilon_9\rho_{2,r}}, \varepsilon_7 = 0, \\ &\delta_1 = -\frac{\delta_5\varepsilon_8}{\varepsilon_9}, \delta_3 = \frac{-\delta_2\delta_5\varepsilon_8^2 - \delta_4^2\varepsilon_9^2}{\delta_4\varepsilon_8\varepsilon_9}. \end{aligned} \tag{5.3}$$

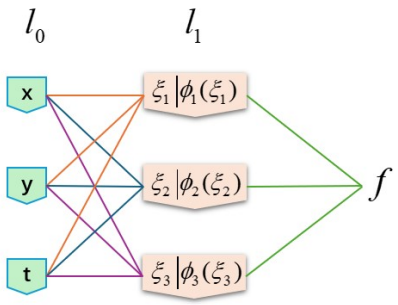

Figure 9. "3-3-1" model for Eq (2.1).

Based on transformation Eq (1.3), we substitute Eq (5.2) into Eq (5.1) and derive an interaction solution as follows:

$$w_6 = \frac{2\varepsilon_7^2\varepsilon_3^3\rho_{1,r}\rho_{3,r}e^{b_3+\varepsilon_7 x+\varepsilon_8 y} + 4\varepsilon_4^2\varepsilon_3\rho_{2,r}\left(\varepsilon_7 x+\varepsilon_8 y\right)\left(\varepsilon_3^2\rho_{1,r}+\varepsilon_6^2\rho_{2,r}\right)+\psi_3}{a\varepsilon_7\varepsilon_3^3\rho_{1,r}+\varepsilon_7\varepsilon_3^3\rho_{1,r}\rho_{3,r}e^{b_3+\varepsilon_7 x+\varepsilon_8 y}+\varepsilon_7\varepsilon_3^3\psi_1^2\rho_{1,r}^2+\varepsilon_7\varepsilon_3^3\psi_2^2\rho_{1,r}\rho_{2,r}}, \tag{5.4}$$

where

$$\begin{cases} \psi_1 = -\frac{\varepsilon_4\varepsilon_6\rho_{2,r}}{\varepsilon_3\rho_{1,r}}x + b_1 + \varepsilon_3 t + \varepsilon_2 y, \\ \psi_2 = \frac{\varepsilon_4\varepsilon_8\varepsilon_6^2\rho_{2,r}}{\varepsilon_3^2\varepsilon_7\rho_{1,r}}y + b_2 + \varepsilon_6 t + \varepsilon_4 x + \frac{\varepsilon_2\varepsilon_6}{\varepsilon_3}y + \frac{\varepsilon_4\varepsilon_8}{\varepsilon_7}y, \\ \psi_3 = 4b_2\varepsilon_3^3\varepsilon_4\varepsilon_7\rho_{1,r}\rho_{2,r} - 4b_1\varepsilon_3^2\varepsilon_4\varepsilon_6\varepsilon_7\rho_{1,r}\rho_{2,r}. \end{cases} \tag{5.5}$$

Then, after inserting Eq (5.3) into Eq (5.1), we obtain another interaction solution as shown below:

$$w_7 = \frac{4\delta_4\left(\varepsilon_3\varepsilon_8-\varepsilon_2\varepsilon_9\right)\rho_{1,r}\left(\delta_4\varepsilon_9\left(\varepsilon_3\varepsilon_8-\varepsilon_2\varepsilon_9\right)\left(\varepsilon_3^2\rho_{1,r}+\varepsilon_6^2\rho_{2,r}\right)x+\delta_2\varepsilon_8\psi_2\right)}{\delta_2^2\varepsilon_6^2\varepsilon_8^2\varepsilon_9\rho_{2,r}\left(\rho_{3,r}e^{b_3+\varepsilon_9 t+\varepsilon_8 y}+\psi_1^2\rho_{1,r}+\psi_3^2\rho_{2,r}+a\right)}, \tag{5.6}$$

where

$$\begin{cases} \psi_1 = b_1 + \varepsilon_3 t + \frac{\delta_4\varepsilon_2\varepsilon_9}{\delta_2\varepsilon_8}x - \frac{\delta_4\varepsilon_3}{\delta_2}x + \varepsilon_2 y, \\ \psi_2 = \varepsilon_8\varepsilon_3^3\rho_{1,r}y - \varepsilon_2\varepsilon_9\varepsilon_3^2\rho_{1,r}y - \psi_4, \\ \psi_3 = -\frac{\varepsilon_2\varepsilon_3\rho_{1,r}}{\varepsilon_6\rho_{2,r}}y + b_2 + \varepsilon_6 t + \psi_5 + \frac{\varepsilon_6\varepsilon_8}{\varepsilon_9}y, \\ \psi_4 = \varepsilon_9\varepsilon_6^2\rho_{2,r}\left(b_1+\varepsilon_2 y\right) + \varepsilon_3\varepsilon_6\rho_{2,r}\left(b_2\varepsilon_9+\varepsilon_6\varepsilon_8 y\right), \\ \psi_5 = \frac{\delta_4\varepsilon_3^2\rho_{1,r}}{\delta_2\varepsilon_6\rho_{2,r}}x - \frac{\delta_4\varepsilon_2\varepsilon_9\varepsilon_3\rho_{1,r}}{\delta_2\varepsilon_6\varepsilon_8\rho_{2,r}}x + \frac{\varepsilon_8\varepsilon_3^2\rho_{1,r}}{\varepsilon_6\varepsilon_9\rho_{2,r}}y. \end{cases} \tag{5.7}$$

To display the interaction phenomenon, we select appropriate parameters and depict the three-dimensional, density, and curve plots as shown in Figures 10 and 11. Both solutions present a multi-crest and multi-trough spatial distribution with a distinct torque-shaped core [40], a hallmark of the nonlinear interaction between the localized lump wave and the propagating exponential wave. Figure 10(c) shows that the symmetry of the crest-trough pairs about the origin when the time variable takes opposite values. In contrast, Figure 11(c) displays a directional propagation tendency toward the origin along the y-axis. Moreover, in the density plots, we can see the clear interference fringes and the dynamic profile

evolution, which manifest the mutual modulation of the spatial confinement of the localized lump and the extended propagation of the exponential wave, which is the intrinsic physical manifestation of the balance between nonlinearity and dispersion [9]. Furthermore, if different parameters are selected, the structure of the interaction solutions will change accordingly.

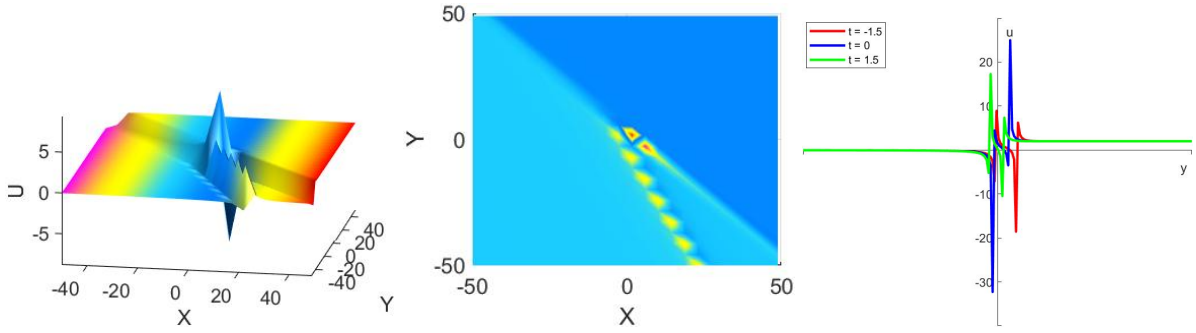

(a) (b) (c)

Figure 10. Interaction solution between the lump and exponential function w_6 with: $\varepsilon_2 = -1, \varepsilon_3 = 2, \varepsilon_4 = 1, \varepsilon_6 = -1, \varepsilon_7 = 1, \varepsilon_8 = 1, \rho_{1,r} = -\frac{1}{2}, \rho_{2,r} = 2, \rho_{3,r} = -1, a = 3, b_1 = -1, b_2 = 1, b_3 = -1, t = 1$. (a): Three-dimensional plot; (b): density plot; (c): curve plots.

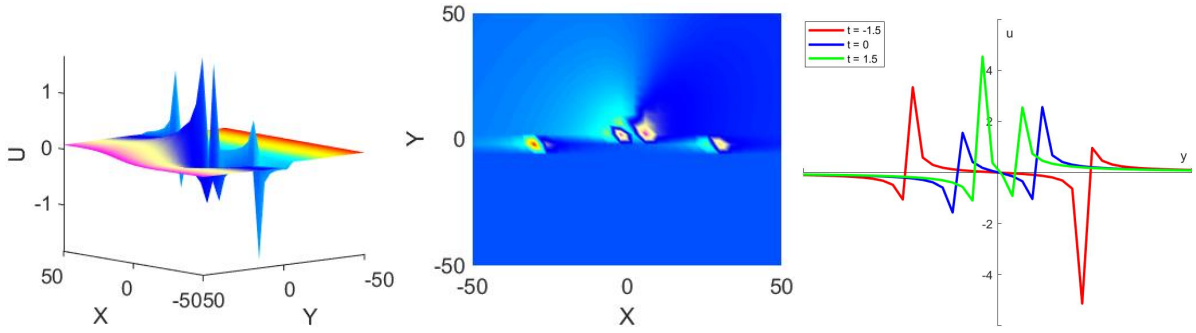

(a) (b) (c)

Figure 11. Interaction solution between the lump and exponential function w_7 with: $\varepsilon_2 = 2, \varepsilon_3 = -2, \varepsilon_6 = 3, \varepsilon_8 = -1, \varepsilon_9 = 2, \delta_2 = -1, \delta_4 = -2, \rho_{1,r} = 1, \rho_{2,r} = 2, \rho_{3,r} = -2, a = 3, b_1 = 2, b_2 = -1, b_3 = 3, t = 2$. (a): Three-dimensional plot; (b): density plot; (c): curve plots.

6. Conclusions

This article concentrates on obtaining the exact solutions of the (2+1)-dimensional gHSISWW-like equation via the bilinear neural network method. As far as we know, few scholars have investigated the exact solutions of this equation. By constructing "3-2-3-1", "3-2-2-1", and "3-3-1" models, we successfully derive the three-wave solutions, rogue wave solutions, and interaction solutions between the lump and exponential function of Eq (1.5). To better present the physical properties of the solutions, we generate three-dimensional, density, and curve figures of the three solutions via MATLAB. From this

article, we can see that the BNNM can effectively derive the exact solutions of NPDEs. In subsequent research, we will extend the BNNM to other nonlinear evolution equations including fractional-order equations and investigate their exact solutions and dynamic behaviors under more general conditions.

Use of AI tools declaration

The authors declare they have not used Artificial Intelligence (AI) tools in the creation of this article.

Acknowledgments

This work is supported in part by the National Natural Science Foundation of China (Nos. 12026263, 12471392, 52472405), Excellent Young and Middle-aged Science and Technology Innovation Team Project of the Education Department of Hubei Province (No. T2022029), Research Ability Cultivation Fund of Hubei University of Arts and Science (No. 2020kypytd006), the Natural Science Foundation of Hubei Province (Nos. 2024AFB202, 2024AFB219, 2024AFD042, 2024AFD045), the Hubei Provincial Department of Education Project (No. B2021211), the International Science and Technology Cooperation Program of Hubei Province (No. 2025EHA017), Hubei Province Central Guiding Local Science and Technology Development Special Project (No. 2024CSA081), Open Fund of Hubei Longzhong Laboratory (No. 2024KF-22), and the Special Fund of Hubei Longzhong Laboratory of Xiangyang Science and Technology Plan.

Conflict of interest

The authors declare there is no conflict of interest.

Author contributions

The first author was responsible for writing the original draft and revising the manuscript. The second author was in charge of writing, reviewing and editing. The third author participated in reviewing and editing the writing. The fourth author participated in reviewing and editing the writing. The fifth author conducted the software implementation.

References

1. R. Hirota, J. Satsuma, Nonlinear evolution equations generated from the Bäcklund transformation for the Boussinesq equation, *Prog. Theor. Phys.*, **57** (1977), 797–807. https://doi.org/10.1143/PTP.57.797
2. Y. D. Shang, Bäcklund transformation, Lax pairs and explicit exact solutions for the shallow water waves equation, *Appl. Math. Comput.*, **187** (2007), 1286–1297. https://doi.org/10.1016/j.amc.2006.09.038
3. M. Wang, G. L. He, T. Xu, Wronskian solutions and N–soliton solutions for the Hirota–Satsuma equation, *Appl. Math. Lett.*, **159** (2025), 109279. https://doi.org/10.1016/j.aml.2024.109279

4. R. Hirota, The direct method in soliton theory, in *Cambridge Tracts in Mathematics* (eds. A. Nagai, J. Nimmo, C. Gilson), Cambridge University Press, (2004). https://doi.org/10.1017/CBO9780511543043
5. R. Hirota, J. Satsuma, N-Soliton solutions of model equations for shallow water waves, *J. Phys. Soc. Jpn.*, **40** (1976), 611–612. https://doi.org/10.1143/JPSJ.40.611
6. Y. N. An, R. Guo, The mixed solutions of the (2+1)-dimensional Hirota–Satsuma–Ito equation and the analysis of nonlinear transformed waves, *Nonlinear Dyn.*, **111** (2023), 18291–18311. https://doi.org/10.1007/s11071-023-08791-2
7. C. Yue, D. C. Lu, M. M. A. Khater, Abundant wave accurate analytical solutions of the fractional nonlinear Hirota–Satsuma–Shallow water wave equation, *Fluids*, **6** (2021), 235. https://doi.org/10.3390/fluids6070235
8. Z. L. Zhao, Y. F. Zhang, Periodic wave solutions and asymptotic analysis of the Hirota–Satsuma shallow water wave equation, *Math. Meth. Appl. Sci.*, **38** (2014), 4262–4271. https://doi.org/10.1002/mma.3362
9. W. X. Ma, J. Li, C. M. Khalique, A study on Lump solutions to a generalized Hirota-Satsuma-Ito equation in (2+1)-dimensions, *Complexity*, **7** (2018), 9059858. https://doi.org/10.1155/2018/9059858
10. Y. Q. Liu, X. Y. Wen, D. S. Wang, The N-soliton solution and localized wave interaction solutions of the (2+1)-dimensional generalized Hirota-Satsuma-Ito equation, *Comput. Math. Appl.*, **77** (2019), 947–966. https://doi.org/10.1016/j.camwa.2018.10.035
11. S. Khaliq, S. Ahmad, A. Ullah, H. Ahmad, S. Saifullah, T. A. Nofal, New waves solutions of the (2+1)-dimensional generalized Hirota–Satsuma–Ito equation using a novel expansion method, *Results. Phys.*, **50** (2023), 106450. https://doi.org/10.1016/j.rinp.2023.106450
12. C. Wang, Y. Shi, W. A. Yang, X. P. Xin, Darboux transformations and exact solutions of nonlocal Kaup–Newell equations with variable coefficients, *Appl. Math. Lett.*, **163** (2025), 109456. https://doi.org/10.1016/j.aml.2025.109456
13. G. H. Wang, The multi-soliton solutions of another two-component Camassa–Holm equation with Darboux transformation approach, *Wave Motion*, **31** (2024), 103396. https://doi.org/10.1016/j.wavemoti.2024.103396
14. J. C. Pu, Y. Chen, Darboux transformation-based LPNN generating novel localized wave solutions, *Physica D*, **467** (2024), 134262. https://doi.org/10.1016/j.physd.2024.134262
15. M. Musette, Painlevé analysis for nonlinear partial differential equations, in *The Painlevé Property* (eds. R. Conte), Springer, New York, NY, (1999), 517–572. https://doi.org/10.1007/978-1-4612-1532-5
16. J. Satsuma, Hirota bilinear method for nonlinear evolution equations, in *Direct and Inverse Methods in Nonlinear Evolution Equations: Lectures Given at the C.I.M.E. Summer School Held in Cetraro, Italy, September 5–12, 1999,* Springer Berlin, Heidelberg, **632** (2003), 171–222. https://doi.org/10.1007/b13714

17. W. J. Yang, K. L. Liu, B. Tang, S. J. Deng, F. Y. Lv, Three wave solution and lump-type solution to a (3+1)-dimensional Date-Jimbo-Kashiwara-Miwa equation with some variable coefficients in inhomogeneous media, *Networks Heterogen. Media*, **20** (2025), 955–969. https://doi.org/10.3934/nhm.2025041

18. Y. S. Bai, Y. N. Liu, W. X. Ma, Lie symmetry analysis, exact solutions, and conservation laws to multi-component nonlinear Schrödinger equations, *Nonlinear Dyn.*, **111** (2023), 18439–18448. https://doi.org/10.1007/s11071-023-08833-9

19. U. H. M. Zaman, M. A. Arefin, M. A. Akbar, M. H. Uddin, Comprehensive dynamic-type multi-soliton solutions to the fractional order nonlinear evolution equation in ocean engineering, *Ain. Shams. Eng. J.*, **15** (2024), 102935. https://doi.org/10.1016/j.asej.2024.102935

20. D. Chou, S. M. Boulaaras, H. U. Rehman, I. Iqbal, A. Akram, N. Ullah, Additional investigation of the Biswas–Arshed equation to reveal optical soliton dynamics in birefringent fiber, *Opt. Quant. Electron.*, **56** (2024), 705. https://doi.org/10.1007/s11082-024-06366-y

21. D. Chou, H. U. Rehman, A. Amer, A. Amer, New solitary wave solutions of generalized fractional Tzitzéica-type evolution equations using Sardar sub-equation method, *Opt. Quant. Electron.*, **55** (2023), 1148. https://doi.org/10.1007/s11082-023-05425-0

22. J. Ahmad, S. Rani, N. B. Turki, N. A. Shah, Novel resonant multi-soliton solutions of time fractional coupled nonlinear Schrödinger equation in optical fiber via an analytical method, *Results. Phys.*, **52** (2023), 106761. https://doi.org/10.1016/j.asej.2024.102935

23. R. F. Zhang, S. Bilige, Bilinear neural network method to obtain the exact analytical solutions of nonlinear partial differential equations and its application to p-gBKP equation, *Nonlinear Dyn.*, **95** (2019), 1–8. https://doi.org/10.1007/s11071-018-04739-z

24. R. F. Zhang, M. C. Li, Bilinear residual network method for solving the exactly explicit solutions of nonlinear evolution equations, *Nonlinear Dyn.*, **108** (2022), 521–531. https://doi.org/10.1007/s11071-022-07207-x

25. M. Zeynel, E. Yaşar, A new (3 + 1) dimensional Hirota bilinear equation: Periodic, rogue, bright and dark wave solutions by bilinear neural network method, *J. Ocean. Eng. Sci.*, (2022), 2468–0133. https://doi.org/10.1016/j.joes.2022.04.017

26. J. G. Liu, W. H. Zhu, Y. K. Wu, G. H. Jin, Application of multivariate bilinear neural network method to fractional partial differential equations, *Results. Phys.*, **47** (2023), 106341. https://doi.org/10.1016/j.rinp.2023.106341

27. Z. H. Zhang, J. G. Liu, A fourth-order nonlinear equation studied by using a multivariate bilinear neural network method, *Nonlinear Dyn.*, **112** (2024), 10229–10237. https://doi.org/10.1007/s11071-024-09567-y

28. J. W. Wang, Y. Q. Liu, L. M. Yan, K. L. Han, L. B. Feng, R. F. Zhang, Fractional sub-equation neural networks (fSENNs) method for exact solutions of space-time fractional partial differential equations, *Chaos*, **35** (2025), 043110. https://doi.org/10.1063/5.0259937

29. H. W. Zhang, R. F. Zhang, Q. R. Liu, A novel Multi-Modal neurosymbolic reasoning intelligent algorithm for BLMP equation, *Chinese Phys. Lett.*, **42** (2025), 100002. https://doi.org/10.1088/0256-307X/42/10/100002

30. X. R. Xie, R. F. Zhang, Neural network-based symbolic calculation approach for solving the Korteweg–de Vries equation, *Chaos, Solitons Fractals*, **194** (2025), 116232. https://doi.org/10.1016/j.chaos.2025.116232

31. Y. H. Yin, X. Lü, S. K. Li, L. X. Yang, Z. Y. Gao, Graph representation learning in the ITS: Car-following informed spatiotemporal network for vehicle trajectory predictions, *IEEE Trans. Intell. Veh.*, **10** (2025), 2642–2652. https://doi.org/10.1109/TIV.2024.3381990

32. Y. H. Yin, X. Lü, S. K. Li, L. X. Yang, Z. Y. Gao, Car-following informed neural networks for real-time vehicle trajectory imputation and prediction, *Transportmetrica A: Transport Sci.*, **22** (2026), 116232. https://doi.org/10.1080/23249935.2024.2374523

33. Y. Chen, X. Lü, H. Tian, R. H. Li, Physics-informed neural network for barrier option pricing in coupled financial quantitative system with varying interest rate and volatility, *Eng. Anal. Bound. Elem.*, **180** (2025), 106457. https://doi.org/10.1016/j.enganabound.2025.106457

34. Y. Chen, X. Lü, X. J. Jia, H. Tian, Barrier option pricing and volatility surface predicting with an extended physics-informed neural network, *Expert. Syst. Appl.*, **291** (2025), 128279. https://doi.org/10.1016/j.eswa.2025.128279

35. M. H. Guo, X. Lü, Y. X. Jin, Extraction and reconstruction of variable-coefficient governing equations using Res-KAN integrating sparse regression, *Physica D*, **481** (2025), 134689. https://doi.org/10.1016/j.physd.2025.134689

36. C. Han, X. Lü, Variable coefficient-informed neural network for PDE inverse problem in fluid dynamics, *Physica D*, **472** (2025), 134362. https://doi.org/10.1016/j.physd.2024.134362

37. Y. B. Su, X. Lü, S. K. Li, L. X. Yang, Z. Y. Gao, Self-adaptive equation embedded neural networks for traffic flow state estimation with sparse data, *Phys. Fluids.*, **36** (2024), 104127. https://doi.org/10.1063/5.0230757

38. W. X. Ma, Generalized bilinear differential equations, *Stud. Nonlinear Sci.*, **2** (2011), 140–144.

39. W. X. Ma, Bilinear equations, Bell polynomials and linear superposition principle, *J. Phys.: Conf. Ser.*, **411** (2013), 012021. https://doi.org/10.1088/1742-6596/411/1/012021

40. Y. Guo, Y. Chen, J. Manafian, S. Malmir, K. H. Mahmoud, A. SA. Alsubaie, Exploring N-soliton solutions, multiple rogue wave and the linear superposition principle to the generalized hirota satsuma-ito equation, *Sci. Rep.*, **14** (2024), 26171. https://doi.org/10.1038/s41598-024-74333-4

41. K. L. Liu, W. J. Yang, B. Tang, New solutions of the (3+1)-dimensional combined pKP-BKP equation, *Phys. Lett. A*, **560** (2025), 130941. https://doi.org/10.1016/j.physleta.2025.130941

42. R. F. Zhang, M. C. Li, M. Albishari, F. C. Zheng, Z. Z. Lan, Generalized lump solutions, classical lump solutions and rogue waves of the (2+1)-dimensional Caudrey-Dodd-Gibbon-Kotera-Sawada-like equation, *Appl. Math. Comput.*, **403** (2021), 126201. https://doi.org/10.1016/j.amc.2021.126201

43. D. P. Rijnsdorp, P. B. Smit, R. T. Guza, A nonlinear, non-dispersive energy balance for surfzone waves: Infragravity wave dynamics on a sloping beach, *J. Fluid. Mech.*, **944** (2022), A45. https://doi.org/10.1017/jfm.2022.512

Appendix A

Based on Eqs (3.19)–(3.21) in reference [39], Eq (1.5) can be derived from Eq (1.4). The derivation is given below:

Step 1: From transformation Eq (1.3), we obtain $f = \mathrm{e}^{\frac{\int w\,dx}{2}}$.

Step 2: By applying the procedure shown in $\left[\frac{T}{f^2}\right]_x$ to both sides of Eq (1.4), we obtain the following equation after simplification:

$$\begin{aligned}&\delta_5\left(f^2f_{xyy}+2f_xf_y^2-ff_xf_{yy}-2ff_{xy}f_y\right)+\delta_4f^2f_{xxt}+\delta_2f^2f_{xxx}+\\&\delta_3f^2f_{xxy}+2\delta_4f_tf_x^2+\delta_1\left(f_t\left(2f_xf_y-ff_{xy}\right)+f\left(f_x\left(-f_{yt}\right)-f_{xt}f_y+ff_{xyt}\right)\right)-\\&\delta_4ff_tf_{xx}+2\delta_2f_x^3-2\delta_4ff_xf_{xt}-6f_xf_{xt}f_{xx}-3\delta_2ff_xf_{xx}-2\delta_3ff_xf_{xy}+\\&2\delta_3f_x^2f_y+3ff_{xt}f_{xxx}+3ff_{xx}f_{xxt}-\delta_3ff_{xx}f_y=0.\end{aligned}\tag{A1}$$

Step 3: Substituting $f = \mathrm{e}^{\frac{\int w\,dx}{2}}$ into Eq (A1) and simplifying, we can obtain

$$\begin{aligned}&3w^3w_t+w^2\left(9w_x\left(\int w_t\,dx\right)+6w_{xt}\right)+6w_x^2\left(\int w_t\,dx\right)+12w_tw_{xx}+\\&8\delta_4w_x+12w_xw_{xt}+8\delta_2w_{xx}+8\delta_3w_{xy}+8\delta_1w_{yt}+8\delta_5w_{yy}+\\&6w\left(w_{xx}\left(\int w_t\,dx\right)+3w_tw_x\right)=0.\end{aligned}\tag{A2}$$

Step 4: Upon simplification of Eq (A2), we can obtain the equation as follows:

$$\begin{aligned}&3w^3w_t+9w^2w_x\int w_t\,dx+6ww_{xx}\int w_t\,dx+18ww_tw_x+\\&6w_x^2\int w_t\,dx+12w_tw_{xx}+6w^2w_{xt}+12w_xw_{xt}+8\delta_1w_{yt}+\\&8\delta_2w_{xx}+8\delta_3w_{xy}+8\delta_4w_{xt}+8\delta_5w_{yy}=0.\end{aligned}\tag{A3}$$

This is Eq (1.5).

Appendix B

In this section, we provide the Mathematica notebook containing the calculation procedures for all results presented in this paper. They are organized as follow:

(1) The Mathematica code implementing the derivation from Eq (1.4) to Eq (1.5):

Step 1: $T = 3\partial_{x,x}f[x,y,t]\partial_{x,t}f[x,y,t] + \delta_1 f[x,y,t]\partial_{y,t}f[x,y,t] - \delta_1\partial_t f[x,y,t]\partial_y f[x,y,t] + \delta_2 f[x,y,t]\partial_{x,x}f[x,y,t] - \delta_2\partial_x^2 f[x,y,t] + \delta_3 f[x,y,t]\partial_{x,y}f[x,y,t] - \delta_3\partial_x f[x,y,t]\partial_y f[x,y,t] + \delta_4 f[x,y,t]\partial_{x,t}f[x,y,t] - \delta_4\partial_t f[x,y,t]\partial_x f[x,y,t] + \delta_5 f[x,y,t]\partial_{y,y}f[x,y,t] - \delta_5\partial_y^2 f[x,y,t] = 0$

Step 2: Simplify$[\partial_x \frac{T}{f[x,y,t]^2} = 0]$

Step 3: Substituting $f[x,y,t] = \mathrm{e}^{\frac{\int w[x,y,t]\,dx}{2}}$ into Simplify$[\partial_x \frac{T}{f[x,y,t]^2} = 0]$

(2) The Mathematica code implementing the derivation of Eqs (3.2) and (3.3):

Step 1:

$$\xi_1 = b_1 + \varepsilon_3 t + \varepsilon_1 x + \varepsilon_2 y$$
$$\xi_2 = b_2 + \varepsilon_6 t + \varepsilon_4 x + \varepsilon_5 y$$
$$\xi_3 = \xi_1\rho_{3,1} + \xi_2\rho_{3,2} + b_3$$
$$\xi_4 = \xi_1\rho_{4,1} + \xi_2\rho_{4,2} + b_4$$
$$\xi_5 = \xi_1\rho_{5,1} + \xi_2\rho_{5,2} + b_5$$
$$f = Exp[\xi_3]\rho_{3,r} + Exp[-\xi_3]\rho_{4,r} + Sin[\xi_4]\rho_{5,r} + Cos[\xi_5]\rho_{6,r} + a$$

poly1 = Expand$[3\partial_{x,x}f\partial_{x,t}f + \delta_1 f\partial_{y,t}f - \delta_1\partial_t f\partial_y f + \delta_2 f\partial_{x,x}f - \delta_2\partial_x^2 f + \delta_3 f\partial_{x,y}f - \delta_3\partial_x f\partial_y f + \delta_4 f\partial_{x,t}f - \delta_4\partial_t f\partial_x f + \delta_5 f\partial_{y,y}f - \delta_5\partial_y^2 f]$

Step 2: poly2 = poly1 $/.\, Sin[\rho_{4,1}(b_1 + t\varepsilon_3 + x\varepsilon_1 + y\varepsilon_2) + \rho_{4,2}(b_2 + t\varepsilon_6 + x\varepsilon_4 + y\varepsilon_5) + b_4]^2 \to 1 - Cos[\rho_{4,1}(b_1 + t\varepsilon_3 + x\varepsilon_1 + y\varepsilon_2) + \rho_{4,2}(b_2 + t\varepsilon_6 + x\varepsilon_4 + y\varepsilon_5) + b_4]^2$

Step 3:

poly3 = Collect[poly2,M]

M is follows:

$\mathrm{e}^{\rho_{3,1}(b_1+\varepsilon_3 t+\varepsilon_1 x+\varepsilon_2 y)+\rho_{3,2}(b_2+\varepsilon_6 t+\varepsilon_4 x+\varepsilon_5 y)+b_3}$,

$\mathrm{e}^{-\rho_{3,1}(b_1+\varepsilon_3 t+\varepsilon_1 x+\varepsilon_2 y)-\rho_{3,2}(b_2+\varepsilon_6 t+\varepsilon_4 x+\varepsilon_5 y)-b_3}$,

$\mathrm{e}^{2\rho_{3,1}(b_1+\varepsilon_3 t+\varepsilon_1 x+\varepsilon_2 y)+2\rho_{3,2}(b_2+\varepsilon_6 t+\varepsilon_4 x+\varepsilon_5 y)+2b_3}$,

$\mathrm{e}^{-2\rho_{3,1}(b_1+\varepsilon_3 t+\varepsilon_1 x+\varepsilon_2 y)-2\rho_{3,2}(b_2+\varepsilon_6 t+\varepsilon_4 x+\varepsilon_5 y)-2b_3}$,

$Sin[\rho_{4,1}(b_1 + \varepsilon_3 t + \varepsilon_1 x + \varepsilon_2 y) + \rho_{4,2}(b_2 + \varepsilon_6 t + \varepsilon_4 x + \varepsilon_5 y) + b_4]$,

$Cos[\rho_{4,1}(b_1 + \varepsilon_3 t + \varepsilon_1 x + \varepsilon_2 y) + \rho_{4,2}(b_2 + \varepsilon_6 t + \varepsilon_4 x + \varepsilon_5 y) + b_4]$,

$Sin[\rho_{5,1}(b_1 + \varepsilon_3 t + \varepsilon_1 x + \varepsilon_2 y) + \rho_{5,2}(b_2 + \varepsilon_6 t + \varepsilon_4 x + \varepsilon_5 y) + b_5]$,

$Cos[\rho_{5,1}(b_1 + \varepsilon_3 t + \varepsilon_1 x + \varepsilon_2 y) + \rho_{5,2}(b_2 + \varepsilon_6 t + \varepsilon_4 x + \varepsilon_5 y) + b_5]$

Step 4:

Solve[A,B], where A is the system of equations formed by setting all coefficients of poly3 to zero and B is the solution parameter chosen for Eqs (3.2) and (3.3).

(3) The Mathematica code implementing the derivation of Eq (3.4):

Step 1:

$$\varepsilon_1 = -\frac{\varepsilon_4\rho_{3,2}}{\rho_{3,1}}, \varepsilon_2 = -\frac{\varepsilon_5\rho_{3,2}}{\rho_{3,1}}, \varepsilon_6 = -\frac{\varepsilon_3\rho_{4,1}}{\rho_{4,2}}, \delta_3 = \frac{-\delta_2\varepsilon_4^2 - \delta_5\varepsilon_5^2}{\varepsilon_4\varepsilon_5}, \delta_4 = -\frac{\delta_1\varepsilon_5}{\varepsilon_4}, \rho_{5,2} = \frac{\rho_{3,2}\rho_{5,1}}{\rho_{3,1}}$$
$$\xi_1 = b_1 + \varepsilon_3 t + \varepsilon_1 x + \varepsilon_2 y$$
$$\xi_2 = b_2 + \varepsilon_6 t + \varepsilon_4 x + \varepsilon_5 y$$
$$\xi_3 = \xi_1\rho_{3,1} + \xi_2\rho_{3,2} + b_3$$

$\xi_4 = \xi_1\rho_{4,1} + \xi_2\rho_{4,2} + b_4$

$\xi_5 = \xi_1\rho_{5,1} + \xi_2\rho_{5,2} + b_5$

$f = Exp[\xi_3]\rho_{3,r} + Exp[-\xi_3]\rho_{4,r} + Sin[\xi_4]\rho_{5,r} + Cos[\xi_5]\rho_{6,r} + a$

w_1=Simplify[$2\frac{\partial_x f}{f}$]

Step 2:

$\Omega_1 = b_1\rho_{4,1} + b_2\rho_{4,2} + \varepsilon_4\rho_{4,2}x - \frac{\varepsilon_4\rho_{3,2}\rho_{4,1}}{\rho_{3,1}}x + \varepsilon_5\rho_{4,2}y - \frac{\varepsilon_5\rho_{3,2}\rho_{4,1}}{\rho_{3,1}}y + b_4$

$\Omega_2 = b_1\rho_{5,1} + \frac{b_2\rho_{3,2}\rho_{5,1}}{\rho_{3,1}} + \varepsilon_3\rho_{5,1}t - \frac{\rho_{5,1}}{\rho_{3,1}}\Omega_4 + b_5$

$\Omega_3 = e^{b_1\rho_{3,1}+b_2\rho_{3,2}+\varepsilon_3\rho_{3,1}t+\Omega_4+b_3}$

$\Omega_4 = \frac{\varepsilon_3\rho_{3,2}\rho_{4,1}}{\rho_{4,2}}t$

(4) The Mathematica code implementing the derivation of Eq (3.6):

Step 1:

$\varepsilon_3 = -\frac{\varepsilon_6\rho_{5,2}}{\rho_{5,1}}, \varepsilon_4 = -\frac{\varepsilon_1\rho_{3,1}}{\rho_{3,2}}, \varepsilon_5 = \frac{-\delta_5\varepsilon_2\rho_{3,1}\rho_{5,1}-\delta_1\varepsilon_6\rho_{3,2}\rho_{5,1}+\delta_1\varepsilon_6\rho_{3,1}\rho_{5,2}}{\delta_5\rho_{3,2}\rho_{5,1}}$,

$\delta_2 = -\frac{\left(\delta_5\varepsilon_2\rho_{5,1}-\delta_1\varepsilon_6\rho_{5,2}\right)\left(\delta_3\varepsilon_1\rho_{5,1}+\delta_5\varepsilon_2\rho_{5,1}-\delta_1\varepsilon_6\rho_{5,2}\right)}{\delta_5\varepsilon_1^2\rho_{5,1}^2}$,

$\delta_4 = -\frac{\delta_1\left(-\delta_3\varepsilon_1\rho_{5,1}-\delta_5\varepsilon_2\rho_{5,1}+\delta_1\varepsilon_6\rho_{5,2}\right)}{\delta_5\varepsilon_1\rho_{5,1}}, \rho_{4,1} = \frac{\rho_{4,2}\rho_{5,1}}{\rho_{5,2}}$

$\xi_1 = b_1 + \varepsilon_3 t + \varepsilon_1 x + \varepsilon_2 y$

$\xi_2 = b_2 + \varepsilon_6 t + \varepsilon_4 x + \varepsilon_5 y$

$\xi_3 = \xi_1\rho_{3,1} + \xi_2\rho_{3,2} + b_3$

$\xi_4 = \xi_1\rho_{4,1} + \xi_2\rho_{4,2} + b_4$

$\xi_5 = \xi_1\rho_{5,1} + \xi_2\rho_{5,2} + b_5$

$f = Exp[\xi_3]\rho_{3,r} + Exp[-\xi_3]\rho_{4,r} + Sin[\xi_4]\rho_{5,r} + Cos[\xi_5]\rho_{6,r} + a$

w_2=Simplify[$2\frac{\partial_x f}{f}$]

Step 2:

$\Omega_1 = e^{b_1\rho_{3,1}+b_2\rho_{3,2}+\varepsilon_6\rho_{3,2}t-\Omega_6+b_3}$

$\Omega_2 = -\rho_{4,2}(\Omega_4 + \Omega_5) + b_2\rho_{4,2} + b_4$

$\Omega_3 = b_1\rho_{5,1} + b_2\rho_{5,2} + \varepsilon_1\rho_{5,1}x + \varepsilon_2\rho_{5,1}y - \Omega_5\rho_{5,2} + b_5$

$\Omega_4 = -\frac{b_1\rho_{5,1}}{\rho_{5,2}} - \frac{\varepsilon_1\rho_{5,1}}{\rho_{5,2}}x - \frac{\varepsilon_2\rho_{5,1}}{\rho_{5,2}}y$

$\Omega_5 = \frac{\varepsilon_1\rho_{3,1}}{\rho_{3,2}}x - \frac{\delta_1\varepsilon_6\rho_{3,1}\rho_{5,2}}{\delta_5\rho_{3,2}\rho_{5,1}}y + \frac{\varepsilon_2\rho_{3,1}}{\rho_{3,2}}y + \frac{\delta_1\varepsilon_6}{\delta_5}y$

$\Omega_6 = \frac{\varepsilon_6\rho_{3,1}\rho_{5,2}}{\rho_{5,1}}t - \frac{\delta_1\varepsilon_6\rho_{3,1}\rho_{5,2}}{\delta_5\rho_{5,1}}y + \frac{\delta_1\varepsilon_6\rho_{3,2}}{\delta_5}y$

(5) The Mathematica code implementing the derivation of Eq (3.8):

Step 1:

$\xi_1 = b_1 + \varepsilon_3 t + \varepsilon_1 x + \varepsilon_2 y$

$\xi_2 = b_2 + \varepsilon_6 t + \varepsilon_4 x + \varepsilon_5 y$

$\xi_3 = \rho_{3,2}Exp[\xi_2] + \xi_1^2\rho_{3,1} + b_3$

$\xi_4 = \rho_{4,2}Exp[\xi_2] + \xi_1^2\rho_{4,1} + b_4$

$\xi_5 = \rho_{5,2}Exp[\xi_2] + \xi_1^2\rho_{5,1} + b_5$

$f = Exp[\xi_3]\rho_{3,r} + Exp[-\xi_3]\rho_{4,r} + Sin[\xi_4]\rho_{5,r} + Cos[\xi_5]\rho_{6,r} + a$

poly1 = Expand[$3\partial_{x,x}f\partial_{x,t}f + \delta_1 f\partial_{y,t}f - \delta_1\partial_t f\partial_y f + \delta_2 f\partial_{x,x}f - \delta_2\partial_x^2 f + \delta_3 f\partial_{x,y}f - \delta_3\partial_x f\partial_y f + \delta_4 f\partial_{x,t}f - \delta_4\partial_t f\partial_x f + \delta_5 f\partial_{y,y}f - \delta_5\partial_y^2 f$]

Step 2:

poly2 = poly1 /.

$Sin[\rho_{5,1}(b_1 + \varepsilon_3 t + \varepsilon_1 x + \varepsilon_2 y)^2 + \rho_{5,2}e^{b_2+\varepsilon_6 t+\varepsilon_4 x+\varepsilon_5 y} + b_5]^2 \rightarrow$

$1 - Cos[\rho_{5,1}\,(b_1 + \varepsilon_3 t + \varepsilon_1 x + \varepsilon_2 y)^{\,2} + \rho_{5,2} e^{b_2+\varepsilon_6 t+\varepsilon_4 x+\varepsilon_5 y} + b_5]^2,$
$Sin[\rho_{4,1}\,(b_1 + \varepsilon_3 t + \varepsilon_1 x + \varepsilon_2 y)^{\,2} + \rho_{4,2} e^{b_2+\varepsilon_6 t+\varepsilon_4 x+\varepsilon_5 y} + b_4]^2 \rightarrow$
$1 - Cos[\rho_{4,1}\,(b_1 + \varepsilon_3 t + \varepsilon_1 x + \varepsilon_2 y)^{\,2} + \rho_{4,2} e^{b_2+\varepsilon_6 t+\varepsilon_4 x+\varepsilon_5 y} + b_4]^2$

Step 3:

poly3 = poly2 /. $\varepsilon_1 \rightarrow 0, \varepsilon_6 \rightarrow 0, \rho_{3,2} \rightarrow 0, \rho_{4,1} \rightarrow 0, \rho_{5,1} \rightarrow 0$

Step 4:

poly4 = Collect[poly3,M]

M is as follows:

$x, y, t, e^{\rho_{3,1}(b_1+t\varepsilon_3+y\varepsilon_2)^2+b_3}, e^{2\rho_{3,1}(b_1+t\varepsilon_3+y\varepsilon_2)^2+2b_3},$
$e^{-\rho_{3,1}(b_1+t\varepsilon_3+y\varepsilon_2)^2-b_3}, e^{b_2+x\varepsilon_4+y\varepsilon_5}, e^{2b_2+2x\varepsilon_4+2y\varepsilon_5},$
$e^{\rho_{3,1}(b_1+t\varepsilon_3+y\varepsilon_2)^2+b_2+b_3+x\varepsilon_4+y\varepsilon_5}, e^{\rho_{3,1}(b_1+t\varepsilon_3+y\varepsilon_2)^2+2b_2+b_3+2x\varepsilon_4+2y\varepsilon_5},$
$e^{-\rho_{3,1}(b_1+t\varepsilon_3+y\varepsilon_2)^2+b_2-b_3+x\varepsilon_4+y\varepsilon_5}, e^{-\rho_{3,1}(b_1+t\varepsilon_3+y\varepsilon_2)^2+2b_2-b_3+2x\varepsilon_4+2y\varepsilon_5},$
$Sin[\rho_{4,2}e^{b_2+x\varepsilon_4+y\varepsilon_5} + b_4], Cos[\rho_{4,2}e^{b_2+x\varepsilon_4+y\varepsilon_5} + b_4],$
$Sin[\rho_{5,2}e^{b_2+x\varepsilon_4+y\varepsilon_5} + b_5], Cos[\rho_{5,2}e^{b_2+x\varepsilon_4+y\varepsilon_5} + b_5]$

Step 4:

Solve[A,B], where A is the system of equations formed by setting all coefficients of poly4 to zero and B is $\varepsilon_2, \varepsilon_4$, and δ_4.

(6) The Mathematica code implementing the derivation of Eq (3.9):

Step 1:

$\varepsilon_1 = 0, \varepsilon_2 = 0, \varepsilon_4 = \frac{\sqrt{\delta_3^2\varepsilon_5^2 - 4\delta_2\delta_5\varepsilon_5^2} - \delta_3\varepsilon_5}{2\delta_2}, \varepsilon_6 = 0, \delta_4 = \frac{\delta_1\sqrt{(\delta_3^2 - 4\delta_2\delta_5)\varepsilon_5^2} + \delta_3\delta_1\varepsilon_5}{2\delta_5\varepsilon_5},$
$\rho_{3,2} = 0, \rho_{4,1} = 0, \rho_{5,1} = 0,$
$\xi_1 = b_1 + \varepsilon_3 t + \varepsilon_1 x + \varepsilon_2 y$
$\xi_2 = b_2 + \varepsilon_6 t + \varepsilon_4 x + \varepsilon_5 y$
$\xi_3 = \rho_{3,2} Exp[\xi_2] + \xi_1^2 \rho_{3,1} + b_3$
$\xi_4 = \rho_{4,2} Exp[\xi_2] + \xi_1^2 \rho_{4,1} + b_4$
$\xi_5 = \rho_{5,2} Exp[\xi_2] + \xi_1^2 \rho_{5,1} + b_5$
$f = Exp[\xi_3]\rho_{3,r} + Exp[-\xi_3]\rho_{4,r} + Sin[\xi_4]\rho_{5,r} + Cos[\xi_5]\rho_{6,r} + a$
w_3=Simplify[$2\frac{\partial_x f}{f}$]

Step 2:

$\Omega_1 = b_2 + \frac{x\Omega_4}{2\delta_2} + \varepsilon_5 y$
$\Omega_2 = \rho_{4,2}\rho_{5,r}\cos\left(e^{\Omega_1}\rho_{4,2} + b_4\right) - \rho_{5,2}\rho_{6,r}\sin\left(e^{\Omega_1}\rho_{5,2} + b_5\right)$
$\Omega_3 = \rho_{5,r}\sin\left(e^{\Omega_1}\rho_{4,2} + b_4\right) + \rho_{6,r}\cos\left(e^{\Omega_1}\rho_{5,2} + b_5\right)$
$\Omega_4 = \sqrt{\left(\delta_3^2 - 4\delta_2\delta_5\right)\varepsilon_5^2} - \delta_3\varepsilon_5$
$\Omega_5 = \rho_{3,1}\,(b_1 + \varepsilon_3 t)^{\,2} + b_3$

(7) The Mathematica code implementing the derivation of Eq (4.2) and Eq (4.3):

Step 1:

$\xi_1 = b_1 + \varepsilon_3 t + \varepsilon_1 x + \varepsilon_2 y$
$\xi_2 = b_2 + \varepsilon_6 t + \varepsilon_4 x + \varepsilon_5 y$
$\xi_3 = \rho_{3,2} Exp[\xi_2] + \xi_1 \rho_{3,1} + b_3$
$\xi_4 = \rho_{4,2} Exp[\xi_2] + \xi_1 \rho_{4,1} + b_4$
$f = \xi_3^2 \rho_{3,r} + \xi_4^2 \rho_{4,r} + a$

poly1 = Expand[$3\partial_{x,x}f\partial_{x,t}f+\delta_1 f\partial_{y,t}f-\delta_1\partial_t f\partial_y f+\delta_2 f\partial_{x,x}f-\delta_2\partial_x^2 f+\delta_3 f\partial_{x,y}f-\delta_3\partial_x f\partial_y f+\delta_4 f\partial_{x,t}f-\delta_4\partial_t f\partial_x f+\delta_5 f\partial_{y,y}f-\delta_5\partial_y^2 f$]

Step 2:

poly2 = Collect[poly1,$x, y, t, e^{b_2+\varepsilon_6 t+\varepsilon_4 x+\varepsilon_5 y}, e^{2b_2+2\varepsilon_6 t+2\varepsilon_4 x+2\varepsilon_5 y}, e^{3b_2+3\varepsilon_6 t+3\varepsilon_4 x+3\varepsilon_5 y}, e^{4b_2+4\varepsilon_6 t+4\varepsilon_4 x+4\varepsilon_5 y}$]

Step 3:

Solve[A,B], where A is the system of equations formed by setting all coefficients of poly2 to zero and B is the solution parameter chosen for Eq (4.2) and Eq (4.3).

(8) The Mathematica code implementing the derivation of Eq (4.4):

Step 1:

$$\varepsilon_1 = 0, \varepsilon_2 = -\frac{\delta_1\varepsilon_3}{\delta_5}, \varepsilon_4 = -\frac{\delta_4\delta_5\varepsilon_5}{\delta_1\delta_2}, \varepsilon_6 = 0, \delta_3 = \frac{\delta_2\delta_1^2+\delta_4^2\delta_5}{\delta_1\delta_4}, \rho_{3,1} = -\frac{\rho_{4,1}\rho_{4,2}\rho_{4,r}}{\rho_{3,2}\rho_{3,r}}$$
$$\xi_1 = b_1 + \varepsilon_3 t + \varepsilon_1 x + \varepsilon_2 y$$
$$\xi_2 = b_2 + \varepsilon_6 t + \varepsilon_4 x + \varepsilon_5 y$$
$$\xi_3 = \rho_{3,2} Exp[\xi_2] + \xi_1\rho_{3,1} + b_3$$
$$\xi_4 = \rho_{4,2} Exp[\xi_2] + \xi_1\rho_{4,1} + b_4$$
$$f = \xi_3^2\rho_{3,r} + \xi_4^2\rho_{4,r} + a$$
$$w_4 = \text{Simplify}[2\frac{\partial_x f}{f}]$$

Step 2:

$$\Phi_1 = b_3 e^{\Phi_5}\rho_{3,2}\rho_{3,r} + \rho_{3,2}^2\rho_{3,r}e^{b_2+\varepsilon_5 y}$$
$$\Phi_2 = \rho_{4,2}e^{b_2+\varepsilon_5 y} + b_4 e^{\Phi_5}$$
$$\Phi_3 = \rho_{4,2}e^{b_2-\Phi_5+\varepsilon_5 y} + \Phi_6\rho_{4,1} + b_4$$
$$\Phi_4 = \rho_{3,2}e^{b_2-\Phi_5+\varepsilon_5 y} - \frac{\Phi_6\rho_{4,1}\rho_{4,2}\rho_{4,r}}{\rho_{3,2}\rho_{3,r}}$$
$$\Phi_5 = \frac{x(\delta_4\delta_5\varepsilon_5)}{\delta_1\delta_2}$$
$$\Phi_6 = b_1 + \varepsilon_3 t - \frac{y(\delta_1\varepsilon_3)}{\delta_5}$$

(9) The Mathematica code implementing the derivation of Eq (4.6):

Step 1:

$$\varepsilon_2 = \frac{\sqrt{\delta_3^2-4\delta_2\delta_5}\varepsilon_1-\delta_3\varepsilon_1}{2\delta_5}, \varepsilon_3 = 0, \varepsilon_4 = 0, \varepsilon_5 = \frac{\delta_4\sqrt{\delta_3^2-4\delta_2\delta_5}\varepsilon_6-\delta_3\delta_4\varepsilon_6}{2\delta_2\delta_5}, \delta_1 = \frac{\delta_3\delta_4-\delta_4\sqrt{\delta_3^2-4\delta_2\delta_5}}{2\delta_2},$$
$$\rho_{3,2} = -\frac{\rho_{4,1}\rho_{4,2}\rho_{4,r}}{\rho_{3,1}\rho_{3,r}}$$
$$\xi_1 = b_1 + \varepsilon_3 t + \varepsilon_1 x + \varepsilon_2 y$$
$$\xi_2 = b_2 + \varepsilon_6 t + \varepsilon_4 x + \varepsilon_5 y$$
$$\xi_3 = \rho_{3,2} Exp[\xi_2] + \xi_1\rho_{3,1} + b_3$$
$$\xi_4 = \rho_{4,2} Exp[\xi_2] + \xi_1\rho_{4,1} + b_4$$
$$f = \xi_3^2\rho_{3,r} + \xi_4^2\rho_{4,r} + a$$
$$w_5 = \text{Simplify}[2\frac{\partial_x f}{f}]$$

Step 2:

$$\Phi_1 = 2b_3\delta_5\rho_{3,1}\rho_{3,r} + 2\delta_5\varepsilon_1 x\rho_{3,1}^2\rho_{3,r} + \delta_3\varepsilon_1(-y)\rho_{3,1}^2\rho_{3,r}$$
$$\Phi_2 = 2b_4\delta_5\rho_{4,1}\rho_{4,r} + 2\delta_5\varepsilon_1 x\rho_{4,1}^2\rho_{4,r} + \delta_3\varepsilon_1(-y)\rho_{4,1}^2\rho_{4,r}$$
$$\Phi_3 = \rho_{4,1}(b_1 + \Phi_5 + \varepsilon_1 x) + \Phi_6\rho_{4,2} + b_4$$
$$\Phi_4 = \rho_{3,1}(b_1 + \Phi_5 + \varepsilon_1 x) - \frac{\Phi_6(\rho_{4,1}\rho_{4,2}\rho_{4,r})}{\rho_{3,1}\rho_{3,r}} + b_3$$
$$\Phi_6 = e^{b_2+\frac{\Phi_5(\delta_4\varepsilon_6)}{\delta_2}+\varepsilon_6 t}$$
$$\Phi_7 = 2b_1\delta_5\left(\rho_{3,1}^2\rho_{3,r} + \rho_{4,1}^2\rho_{4,r}\right)$$

(10) The Mathematica code implementing the derivation of Eqs (5.2) and (5.3):

Step 1:

$$\xi_1 = \varepsilon_1 x + \varepsilon_2 y + \varepsilon_3 t + b_1$$
$$\xi_2 = \varepsilon_4 x + \varepsilon_5 y + \varepsilon_6 t + b_2$$
$$\xi_3 = \varepsilon_7 x + \varepsilon_8 y + \varepsilon_9 t + b_3$$
$$f = \rho_{1,r}{\xi_1}^2 + \rho_{2,r}{\xi_2}^2 + \rho_{3,r} Exp[\xi_3] + a$$

poly1 = Expand[$3\partial_{x,x}f\partial_{x,t}f + \delta_1 f\partial_{y,t}f - \delta_1\partial_t f\partial_y f + \delta_2 f\partial_{x,x}f - \delta_2\partial_x^2 f + \delta_3 f\partial_{x,y}f - \delta_3\partial_x f\partial_y f + \delta_4 f\partial_{x,t}f - \delta_4\partial_t f\partial_x f + \delta_5 f\partial_{y,y}f - \delta_5\partial_y^2 f$]

Step 2:

poly2 = Collect[poly1,$x, y, t, e^{b_3+\varepsilon_9 t+\varepsilon_7 x+\varepsilon_8 y}, e^{2b_3+2\varepsilon_9 t+2\varepsilon_7 x+2\varepsilon_8 y}$]

Step 3:

Solve [A,B], where A is the system of equations formed by setting all coefficients of poly2 to zero and B is the solution parameter chosen for Eqs (5.2) and (5.3).

(11) The Mathematica code implementing the derivation of Eq (5.4):

Step 1:

$$\varepsilon_1 = -\frac{\varepsilon_4\varepsilon_6\rho_{2,r}}{\varepsilon_3\rho_{1,r}}, \varepsilon_5 = \frac{\varepsilon_4\varepsilon_8\varepsilon_3^2\rho_{1,r}+\varepsilon_2\varepsilon_6\varepsilon_7\varepsilon_3\rho_{1,r}+\varepsilon_4\varepsilon_6^2\varepsilon_8\rho_{2,r}}{\varepsilon_3^2\varepsilon_7\rho_{1,r}}, \varepsilon_9 = 0, \delta_1 = \frac{(\delta_2\varepsilon_7+\delta_3\varepsilon_8)\left(\varepsilon_2\varepsilon_3\varepsilon_7\rho_{1,r}+\varepsilon_4\varepsilon_6\varepsilon_8\rho_{2,r}\right)}{\varepsilon_3^2\varepsilon_8^2\rho_{1,r}},$$
$$\delta_4 = \frac{\delta_2\left(\varepsilon_2\varepsilon_3\varepsilon_7\rho_{1,r}+\varepsilon_4\varepsilon_6\varepsilon_8\rho_{2,r}\right)}{\varepsilon_3^2\varepsilon_8\rho_{1,r}}, \delta_5 = \frac{-\delta_2\varepsilon_7^2-\delta_3\varepsilon_8\varepsilon_7}{\varepsilon_8^2},$$
$$\xi_1 = \varepsilon_1 x + \varepsilon_2 y + \varepsilon_3 t + b_1$$
$$\xi_2 = \varepsilon_4 x + \varepsilon_5 y + \varepsilon_6 t + b_2$$
$$\xi_3 = \varepsilon_7 x + \varepsilon_8 y + \varepsilon_9 t + b_3$$
$$f = \rho_{1,r}{\xi_1}^2 + \rho_{2,r}{\xi_2}^2 + \rho_{3,r} Exp[\xi_3] + a$$
$$w_6 = \text{Simplify}[2\tfrac{\partial_x f}{f}]$$

Step 2:

$$\psi_1 = -\frac{\varepsilon_4\varepsilon_6 x\rho_{2,r}}{\varepsilon_3\rho_{1,r}} + b_1 + \varepsilon_3 t + \varepsilon_2 y$$
$$\psi_2 = \frac{\varepsilon_4\varepsilon_8\varepsilon_6^2 y\rho_{2,r}}{\varepsilon_3^2\varepsilon_7\rho_{1,r}} + b_2 + \varepsilon_6 t + \varepsilon_4 x + \frac{\varepsilon_2\varepsilon_6 y}{\varepsilon_3} + \frac{\varepsilon_4\varepsilon_8 y}{\varepsilon_7}$$
$$\psi_3 = 4b_2\varepsilon_3^3\varepsilon_4\varepsilon_7\rho_{1,r}\rho_{2,r} - 4b_1\varepsilon_3^2\varepsilon_4\varepsilon_6\varepsilon_7\rho_{1,r}\rho_{2,r}$$

(12) The Mathematica code implementing the derivation of Eq (5.6):

Step 1:

$$\varepsilon_1 = -\frac{\delta_4(\varepsilon_3\varepsilon_8-\varepsilon_2\varepsilon_9)}{\delta_2\varepsilon_8}, \varepsilon_4 = \frac{\delta_4\varepsilon_3(\varepsilon_3\varepsilon_8-\varepsilon_2\varepsilon_9)\rho_{1,r}}{\delta_2\varepsilon_6\varepsilon_8\rho_{2,r}}, \varepsilon_5 = \frac{\varepsilon_8\varepsilon_3^2\rho_{1,r}-\varepsilon_2\varepsilon_9\varepsilon_3\rho_{1,r}+\varepsilon_6^2\varepsilon_8\rho_{2,r}}{\varepsilon_6\varepsilon_9\rho_{2,r}}, \varepsilon_7 = 0,$$
$$\delta_1 = -\frac{\delta_5\varepsilon_8}{\varepsilon_9}, \delta_3 = \frac{-\delta_2\delta_5\varepsilon_8^2-\delta_4^2\varepsilon_9^2}{\delta_4\varepsilon_8\varepsilon_9},$$
$$\xi_1 = \varepsilon_1 x + \varepsilon_2 y + \varepsilon_3 t + b_1$$
$$\xi_2 = \varepsilon_4 x + \varepsilon_5 y + \varepsilon_6 t + b_2$$
$$\xi_3 = \varepsilon_7 x + \varepsilon_8 y + \varepsilon_9 t + b_3$$
$$f = \rho_{1,r}{\xi_1}^2 + \rho_{2,r}{\xi_2}^2 + \rho_{3,r} Exp[\xi_3] + a$$
$$w_7 = \text{Simplify}[2\tfrac{\partial_x f}{f}]$$

Step 2:

$$\psi_1 = b_1 + \varepsilon_3 t + \frac{\delta_4\varepsilon_2\varepsilon_9 x}{\delta_2\varepsilon_8} - \frac{\delta_4\varepsilon_3 x}{\delta_2} + \varepsilon_2 y$$
$$\psi_2 = \varepsilon_8\varepsilon_3^3 y\rho_{1,r} - \varepsilon_2\varepsilon_9\varepsilon_3^2 y\rho_{1,r} - \psi_4$$
$$\psi_3 = -\frac{\varepsilon_2\varepsilon_3 y\rho_{1,r}}{\varepsilon_6\rho_{2,r}} + b_2 + \varepsilon_6 t + \psi_5 + \frac{\varepsilon_6\varepsilon_8 y}{\varepsilon_9}$$
$$\psi_4 = \varepsilon_9\varepsilon_6^2\rho_{2,r}(b_1 + \varepsilon_2 y) + \varepsilon_3\varepsilon_6\rho_{2,r}(b_2\varepsilon_9 + \varepsilon_6\varepsilon_8 y)$$
$$\psi_5 = \frac{\delta_4\varepsilon_3^2 x\rho_{1,r}}{\delta_2\varepsilon_6\rho_{2,r}} - \frac{\delta_4\varepsilon_2\varepsilon_9\varepsilon_3 x\rho_{1,r}}{\delta_2\varepsilon_6\varepsilon_8\rho_{2,r}} + \frac{\varepsilon_8\varepsilon_3^2 y\rho_{1,r}}{\varepsilon_6\varepsilon_9\rho_{2,r}}$$

Appendix C

In this section, we provide the reasoning why the obtained solutions w satisfy Eq (1.5). The detailed verification procedure is as follows:

As an example, we consider the rogue wave solution w_3 in Section 4.

Step 1: For the rogue wave solution w_3 in Section 4, based on transformation Eq (1.3), we obtain $f = \mathrm{e}^{\frac{\int w_3\, dx}{2}}$.

Step 2: Verified via Mathematica, we confirm that the function f obtained by substituting Eq (4.2) into Eq (4.1) satisfies Eq (1.4). Therefore, the function f obtained also satisfies $\left[\frac{T}{f^2}\right]_x = 0$. The detailed Mathematica verification code can be found in Appendix B.

Step 3: According to Appendix A, Eq (1.5) is obtained by substituting $f = \mathrm{e}^{\frac{\int w\, dx}{2}}$ into Eq $\left[\frac{T}{f^2}\right]_x = 0$ followed by simplification.

Step 4: Therefore, in Step 1, the function f obtained by substituting w_3 ensures that equation $\left[\frac{T}{f^2}\right]_x = 0$ holds, which further verifies that w_3 satisfies Eq (1.5).

Remark: The verification that other solutions w satisfy Eq (1.5) follows the same steps as above.

AIMS Press